DTU Library

Response of Tibetan Plateau lakes to climate change - Trends, patterns, and mechanisms

Zhang, Guoqing; Yao, Tandong; Xie, Hongjie; Yang, Kun; Zhu, Liping; Shum, C. K.; Bolch, Tobias; Yi, Shuang; Allen, Simon; Jiang, Liguang

Total number of authors:
12

Published in:
Earth-Science Reviews

Link to article, DOI:
10.1016/j.earscirev.2020.103269

Publication date:
2020

Document Version
Peer reviewed version

Response of Tibetan Plateau's lakes to climate changes: Trend, pattern, and mechanisms

Guoqing Zhang[1,2], Tandong Yao[1,2], Hongjie Xie[3], Kun Yang[2,4], Liping Zhu[1,2], C.K. Shum[5], Tobias Bolch[6], Shuang Yi[7], Simon Allen[8], Liguang Jiang[9], Wenfeng Chen[1], Changqing Ke[10]

[1] Key Laboratory of Tibetan Environmental Changes and Land Surface Processes, Institute of Tibetan Plateau Research, Chinese Academy of Sciences (CAS), Beijing, China

[2] CAS Center for Excellence in Tibetan Plateau Earth Sciences, Beijing, China

[3] Center for Advanced Measurements in Extreme Environments, University of Texas at San Antonio, San Antonio, Texas, USA

[4] Ministry of Education Key Laboratory for Earth System Modelling, Department of Earth System Science, Tsinghua University, Beijing, China

[5] Division of Geodetic Science, School of Earth Sciences, The Ohio State University, Ohio, USA

[6] School of Geography and Sustainable Development, University of St Andrews, St Andrews, UK

[7] Institute of Geodesy, University of Stuttgart, Stuttgart, Germany

[8] Department of Geography, University of Zurich, Zürich, Switzerland

[9] Department of Environmental Engineering, Technical University of Denmark, Lyngby, Denmark

[10] School of Geography and Ocean Science, Nanjing University, Nanjing, China

Abstract:

The wide distribution of natural lakes over the Tibetan Plateau, the highest and largest plateau on Earth, have received extensive attention due to global warming. In this Review, we examine alpine lake evolution, spatial patterns and driving mechanisms. The changes in lake area, level and volume show a slight decrease from 1976 to the mid-1990s, followed by a continuous rapid increase. The spatial patterns show an overall lake growth in the north of the inner plateau against a reduction in the south, which are accompanied by most of the lakes cooling in the north against warming in the south, and longer ice cover duration in the north compared with the south. The changes in lake temperature are negatively correlated with water level variations and lake ice duration. Enhanced precipitation is the dominant contributor to increased lake water storage, followed by glacier mass loss and permafrost thawing. The decadal lake expansion since the mid-1990s could have been driven by the positive phase of Atlantic Multidecadal Oscillation, and clear inflection points of lake area/level identified in 1997/1998 and 2015/2016 are attributed to strong El Niño events. In the near-term, the lakes will continue to expand. Future interdisciplinary lake studies are urgently required to improve understanding of climate-cryosphere-hydrosphere interactions and water resource management.

Keywords: Tibetan Plateau, lake evolution, remote sensing, climate change, hydrological cycle

* Corresponding author at: Institute of Tibetan Plateau Research, Chinese Academy of Sciences, Beijing, China, E-mail address: guoqing.zhang@itpcas.ac.cn (G. Zhang)

1. Introduction

Lakes are crucial water resources for aquatic and terrestrial ecosystems, agriculture and industrial production, as well as providing recreation and regulating the climate. The contemporary technology to detect and monitor surface and ground water from space has substantially increased the scope and findings of scientific research on lakes (Huang et al., 2018; Pekel et al., 2016; Tapley et al., 2019). There are ~110 million lakes (>0.002 km^2) globally, accounting for ~1.8% of the total land area, ~3.7% of the Earth's non-glaciated land area (Messager et al., 2016; Verpoorter et al., 2014), and ~0.8% of total global non-frozen terrestrial water stocks (Messager et al., 2016). The patterns of change in water body areas vary extensively with geographical location. For example, high-resolution global surface water mapping between 1984 and 2015 reveals that the Aral Sea (Kazakhstan, Uzbekistan) and the Middle East have large permanent surface water loss due to unregulated withdrawal, dams and droughts (Micklin, 1988), but the Tibetan plateau (TP), where there is little human intervention, has an overall water gain (Pekel et al., 2016). The contiguous United States exhibits divergent trends among water bodies between 1984 and 2016, with decreasing trends in the southwest and northwest water-poor regions, but increasing trends in the southeast and far-north Great Plains water-rich regions (Zou et al., 2018). The expansion of lake area on the TP is in clear contrast to the shrinking of lake area on the adjacent Mongolian Plateau during 1970s−2013 (Tao et al., 2015; Zhang et al., 2017b). In China, the number and area of lakes in the TP and Xinjiang had an increasing trend from the 1960s to 2015, while there were decreasing trends in the Inner-Mongolia Plateau and on the Eastern Plain (Ma et al., 2010; Zhang et al., 2019d). In addition to lake area, water level and volume variations can now be routinely monitored using data from satellite radar and laser altimetry missions (Crétaux et al., 2011; 2016; Jiang et al., 2017b; Zhang et al., 2011c). Other satellite data are also now widely used in surface water measurements, to the benefit of many emergent fields of study, including water temperatures and ice phenology (Alsdorf et al., 2007; O'Reilly et al., 2015; Sharma et al., 2019).

The TP is one of the most sensitive areas to global climate change, and exhibits an early warning signal of global warming (Kuang and Jiao, 2016; Liu and Chen, 2000; Liu et al., 2009). The lakes on the TP are widely and densely distributed, with a total area of ~5×10^4 km^2 in 2018 (Zhang et al., 2019c). This is ~1.9% of global lake area (Messager et al., 2016) and 57.2% of China's lake area (Ma et al., 2010; Zhang et al., 2019d). These lakes on the TP are an effective indicator and sentinel of climate changes, because of the absence of direct anthropogenic influence and their dominant distribution in endorheic basins (Figure 1). For example, lake areas and water storage decreased between the 1970s and 1990s, with decreasing precipitation, while they increased after the 1990s with increasing precipitation and air temperature (Kuang and Jiao, 2016; Yang et al., 2017b; Zhang et al., 2017b). The climate on the TP is dominated by westerlies in winter and the Indian monsoon in summer (Maussion et al., 2014). In addition, the East Asian summer monsoon plays a key role in climate change in the northeastern TP (An et al., 2012). These atmospheric circulation systems affect precipitation patterns on the TP (Yao et al., 2012), driving long-term lake evolution and seasonal cycles. Climate change impacts lakes, and in turn, lakes can modify some aspects of regional climate change through land and atmospheric water and heat exchanges (Wu et al., 2019), and then affect evaporation and precipitation, as seen in the Nam Co area (Dai et al., 2017; Wang et al., 2019).

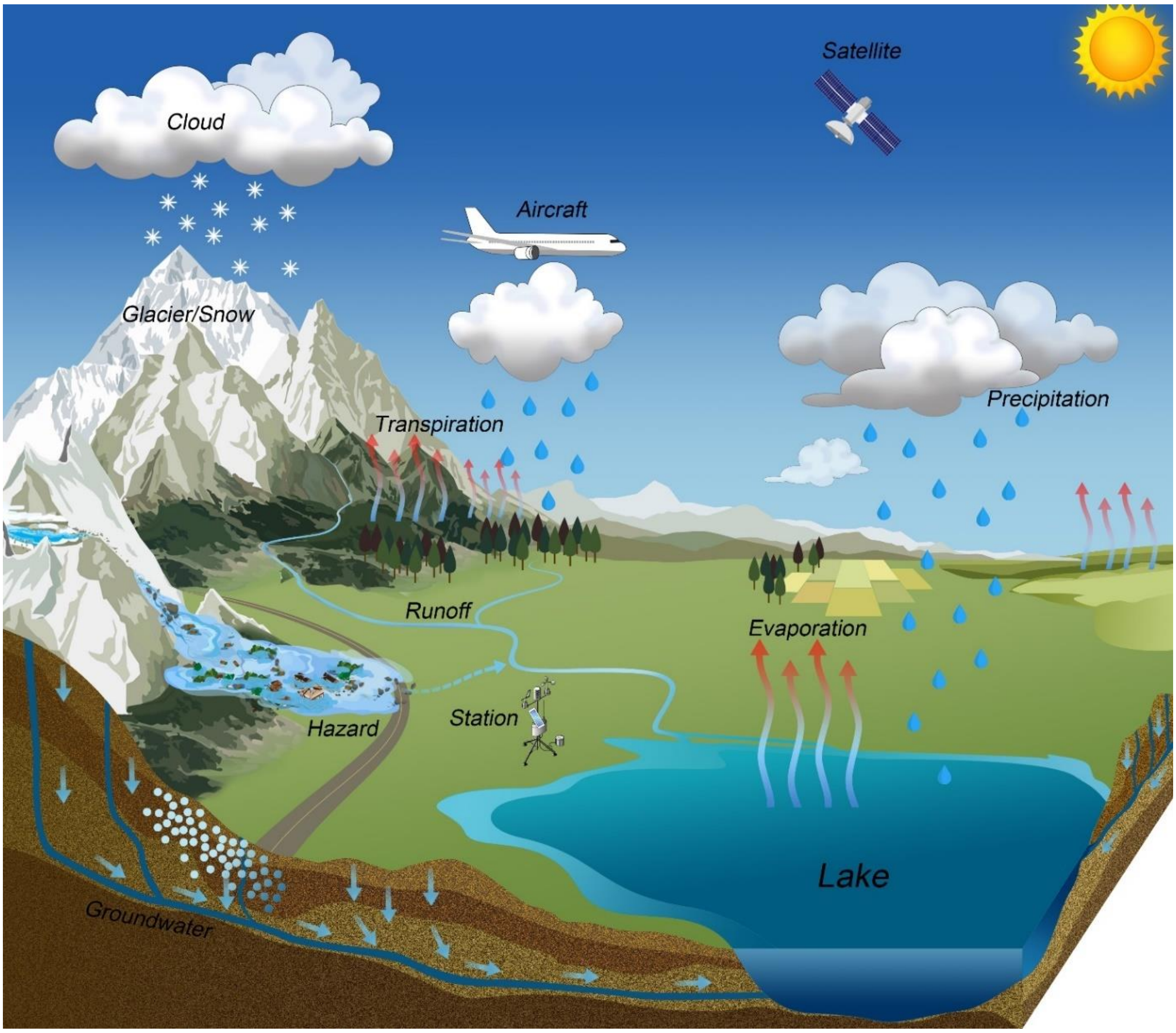

Figure 1. Schematic diagram illustrating key components of lake water balance including precipitation, evaporation, glacier/snow melt and permafrost degradation. Lake observations from satellite, aircraft, and ground-based stations are also shown.

The TP is a vast territory with a sparse population and numerous lakes. Observations of lake changes on the TP include in-situ measurements and widely available remote sensing monitoring. The in-situ investigations and observations can provide detailed hydrological parameters, but are limited in spatial coverage and temporal continuity. For example, lake bathymetry measurements (e.g. Wang et al., 2009; Zhang et al., 2011a) and lake level observations (Lei et al., 2014; Zhang et al., 2011b) are only available for a few large lakes and only for short periods. Although some lake studies have used these first-hand in-situ measurements, they are usually combined with remote sensing data to fill the spatial gaps (Lei et al., 2014; Qiao et al., 2019a; Zhang et al., 2011a). For extensive studies of this vast remote region with its harsh environment, satellite remote sensing is the only practical method, although the data are also limited in high-precision temporal and spatial resolutions, and by the weather and terrain.

A statistical analysis indicates that the number of published articles in international peer-reviewed journals, including all three terms "lake", "Tibetan Plateau", and "remote sensing", increased rapidly between 2000 and 2018, to a current level of ~50 papers per year (Figure 2). Some studies have reviewed lake changes and climate elements over the TP to explain lake water balance. For example, Sun et al. (2018) linked the lake and glacier area changes between 1990 and 2015, and interaction with climate changes such as temperature, precipitation and evaporation. Li et al. (2019b) emphasized multiphase water transformation by characterizing climates (temperature, precipitation), glacier area, depth of permafrost active layers, snowfall/rainfall, and lake area/level changes. Song et al. (2014a) summarized individual lake area changes, and lake level changes during 2003−2009. These studies have qualitatively correlated lake and climate changes during recent decades, but have not explained lake water balance quantitatively.

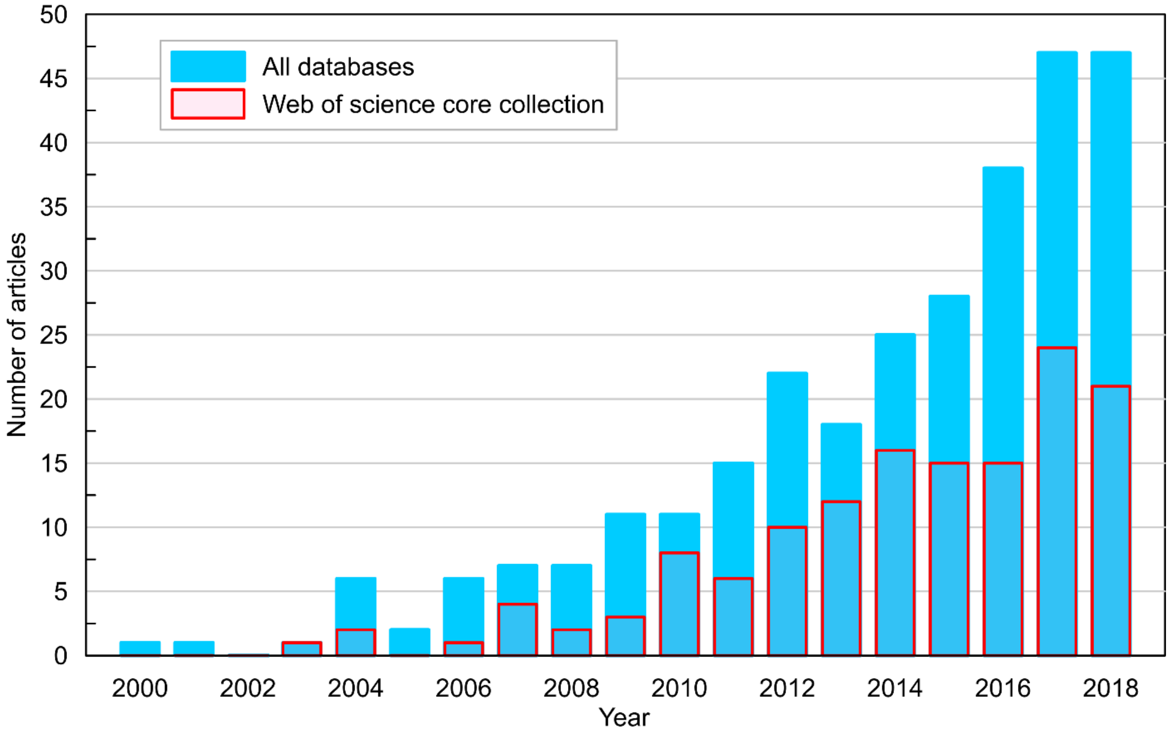

Figure 2. The number of articles published in 2000−2018 derived from the Web of Science for articles including the topics: "lake", "Tibetan Plateau", and "remote sensing".

The large body of literature now available from many lake studies on the TP warrants a comprehensive review to synthesize the current published findings. We summarize the progress of lake studies on the TP and gaps in the research as follows:

- Spatial-temporal monitoring of lake changes has focused on number, area, and volume since the 1970s, driven by the availability of suitable satellite data. However, the differences in the data sources used, and the study periods covered, result in a lack of a comprehensive and systematic picture of lakes from the 1970s to the present, including inter-annual and seasonal variations.

- Lake responses to climate change are reflected not only in number, area and volume, but also in lake surface water temperature and lake ice phenology. The latter have been rarely addressed.
- Regarding the causes of lake changes such as climate (precipitation, evaporation) or cryosphere (glacier, snow, permafrost), qualitative analyses have been the norm. Quantitative examinations of these lakes, in response to local climate changes and/or cryosphere, and lake water balance, are absent.
- Lake evolution and regime shifts may be related to large-scale atmospheric circulations. Investigations of the driving mechanisms behind the lake changes are eagerly awaited.
- Lake changes since the beginning of the satellite era can be observed. Attention should be devoted to the response of lakes to future climate changes.

Here, we present the state of the TP's lakes in response to climate changes, aiming at helping to better understand climate change and the water cycle on the highest and most extensive highland in the world. The knowledge summarized in this review will be of benefit to various research communities such as hydrology, limnology, glaciology, climate change, and remote sensing.

This review is organized as follows. The geographic characteristics of the TP are introduced in Section 2. The applied data and methods of lake mapping, basin-scale mass change and water balance, water surface temperature, and lake ice phenology are described in Section 3. Section 4 presents the results of lake changes in number, area, level and volume, associated with terrestrial water storage (TWS) changes. The responses and feedback of lakes to local climate changes are discussed in Section 5. The response of lakes to large-scale atmospheric circulation and driving mechanisms are presented in Section 6. Section 7 discusses future lake developments, while Section 8 provides a summary of the study, along with recommendations for future studies.

2. Geographic region

The TP is one of the most elevated regions of the Earth, with a mean elevation of ~4000 m above sea level (a.s.l.), and is consequently known as "the Roof of the World". The TP and surroundings (hereafter simply referred to as TP) cover a broad region. In this study we define the TP boundary as the 2,500 m a.s.l. contour (Zhang et al., 2013b), which encloses an area of ~3×10^6 km^2 (Figure 3). The TP has a total glacier area of ~8.3×10^4 km^2 (RGI v6.0) (RGI-Consortium, 2017) and glacier ice storage of ~7.0×10^3 km^3 (Farinotti et al., 2019). This is the largest ice reservoir outside the polar regions, which is why the region is also referred to as "the Third Pole of the Earth" (Qiu, 2008). The TP and its surrounding mountains are also known as "the Water Tower of Asia" (Barnett et al., 2005; Immerzeel et al., 2010) as it is the source for several major Asian rivers such as the Yellow River, the Yangtze, Indus, Ganges, Brahmaputra, Irrawaddy, Salween and Mekong, and provides water to more than a billion people living downstream (Immerzeel et al., 2020). In addition to the glacier coverage, the abundance of natural lakes on the TP (~1400 lakes greater than 1 km^2) (Zhang et al., 2019c) is another important asset, which may have great effects on regional climate and water cycle.

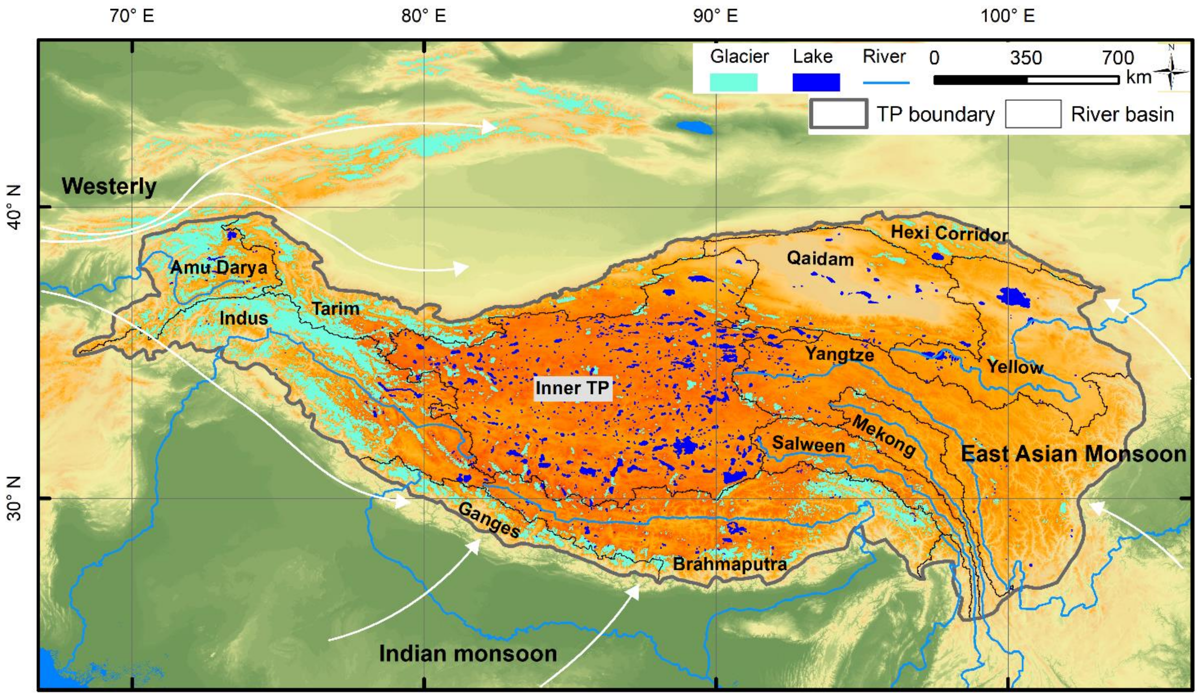

Figure 3. Distribution of lakes (blue), glaciers (light green), and major rivers (Yellow, Yangtze, Mekong, Salween, Brahmaputra, Ganges, and Indus rivers) on the Tibetan Plateau (TP). The TP is divided into 12 large river basins. The large-scale atmospheric circulations such as westerly, India monsoon and East Asian Monsoon are also shown.

The TP encompasses many high mountains, including Mount Everest (8848 m a.s.l.), the highest mountain on Earth. The TP mountains can be classified into two groups: the generally east-west ranges (the Himalaya, the Gangtise-Nyenchen Tanglha, Karakoram Range-Tanggula Mountains, and Kunlun Mountains); and the north-south Hengduan Range. During the monsoon season, the valleys in the Himalaya form the pathways for water vapor from the India Ocean to the TP (Lin et al., 2018). The TP exerts a strong influence on the climate and environmental changes of the Eurasian continent, the formation of the Asian monsoon system and the evolution of the Westerlies through its thermal and dynamical processes (Li, 1999; Liu et al., 2020; Son et al., 2019; Wu et al., 2007).

The annual mean, minimum and maximum air temperature between 1980 and 2018 obtained from the 95 China Meteorological Administration (CMA) (http://data.cma.cn/en) weather stations on the TP are 4.1, 2.8 and 5.1 ^{o}C, respectively. These weather stations show an overall warmer pattern in 1998−2018 relative to 1980−1997 (Figure 4). The average warming rates of these stations are 0.044 ^{o}C/yr during 1980−2018, and 0.031 ^{o}C/yr during 1961−2015, which is greater than the average temperature change in China (0.029 ^{o}C/yr), and two times higher than the rate of global warming (0.014 ^{o}C/yr) during 1961−2015 (Figure S1). The warming of the TP is more significant in winter (Kuang and Jiao, 2016; Liu and Chen, 2000). The increasing rate of the minimum air temperature is twice that of the maximum temperature (Kuang and Jiao, 2016). However, the CMA stations are mainly located in the eastern TP and at relatively low altitudes, while the major lakes are to be found in the vast western TP which has few CMA stations. Some studies

(Guo et al., 2019a; Mountain Research Initiative, 2015; Pepin et al., 2019; Qin et al., 2009) have used the gridded Moderate Resolution Imaging Spectroradiometer (MODIS) land surface temperature (LST) product to estimate elevation-dependent warming, which has the advantage of pixel-based estimation for the whole plateau. The warming rate of satellite-based 2-m air temperature and land surface temperature increases rapidly in areas below ~5000 m a.s.l., but decreases and tends to be stable in areas above 5000 m a.s.l. (Figure S1) (Guo et al., 2019a; Qin et al., 2009). The accelerated warming in the TP has led to rapid glacier retreat, snow melt and permafrost degradation (Bolch et al., 2019; Cheng and Wu, 2007; Guo et al., 2015), affecting the future water resources of the Asian Water Tower (Immerzeel et al., 2020; Yang et al., 2011).

The precipitation records from 95 CMA stations on the TP (Figure 4), with continuous observations after 1980, show annual mean, minimum and maximum precipitation of 482, 418, and 553 mm in 1980−2018, respectively. However, the spatial heterogeneity of precipitation across the TP is apparent (Wang et al., 2018b). For example, the annual summer precipitation decreases gradually from the southeast (~700 mm) to the northeast (~50 mm) (Kang et al., 2010). In addition, the CMA weather station observations show that the elevation dependence of summer precipitation displays an increasing trend between 1970 and 2014 (Li et al., 2017b). Many precipitation products have been produced, evaluated, and utilized, including the Global Precipitation Climatology Centre (GPCC), the Global Precipitation Climatology Project (GPCP), TRMM, the Asian Precipitation-Highly Resolved Observational Data Integration Toward Evaluation of Water Resources (APHRODITE) (Behrangi et al., 2017; Tong et al., 2014; Yang et al., 2014; Yatagai et al., 2012). However, on the TP, these precipitation data sets, derived from satellites and reanalysis, have large uncertainties (seasonal and annual biases) (Behrangi et al., 2017; Tong et al., 2014) and many of them underestimate the precipitation at high elevations (e.g. Wortmann et al., 2018). These uncertainties greatly limit their use in quantitative evaluations of lake water balance in the region. The annual precipitation has a generally increasing trend between 1980 and 2018, especially after 1998 (Figure 4). Most of the stations (99%) reveal an increased precipitation in 1998−2018 relative to 1980−1997, as also seen in reanalysis data (*Sun et al.*, 2020). Overall, the TP is getting warmer and wetter (Kuang and Jiao, 2016), which correlates well with the observed enlargement of lakes (Zhang et al., 2019c) and the greening of vegetation (Zhong et al., 2019).

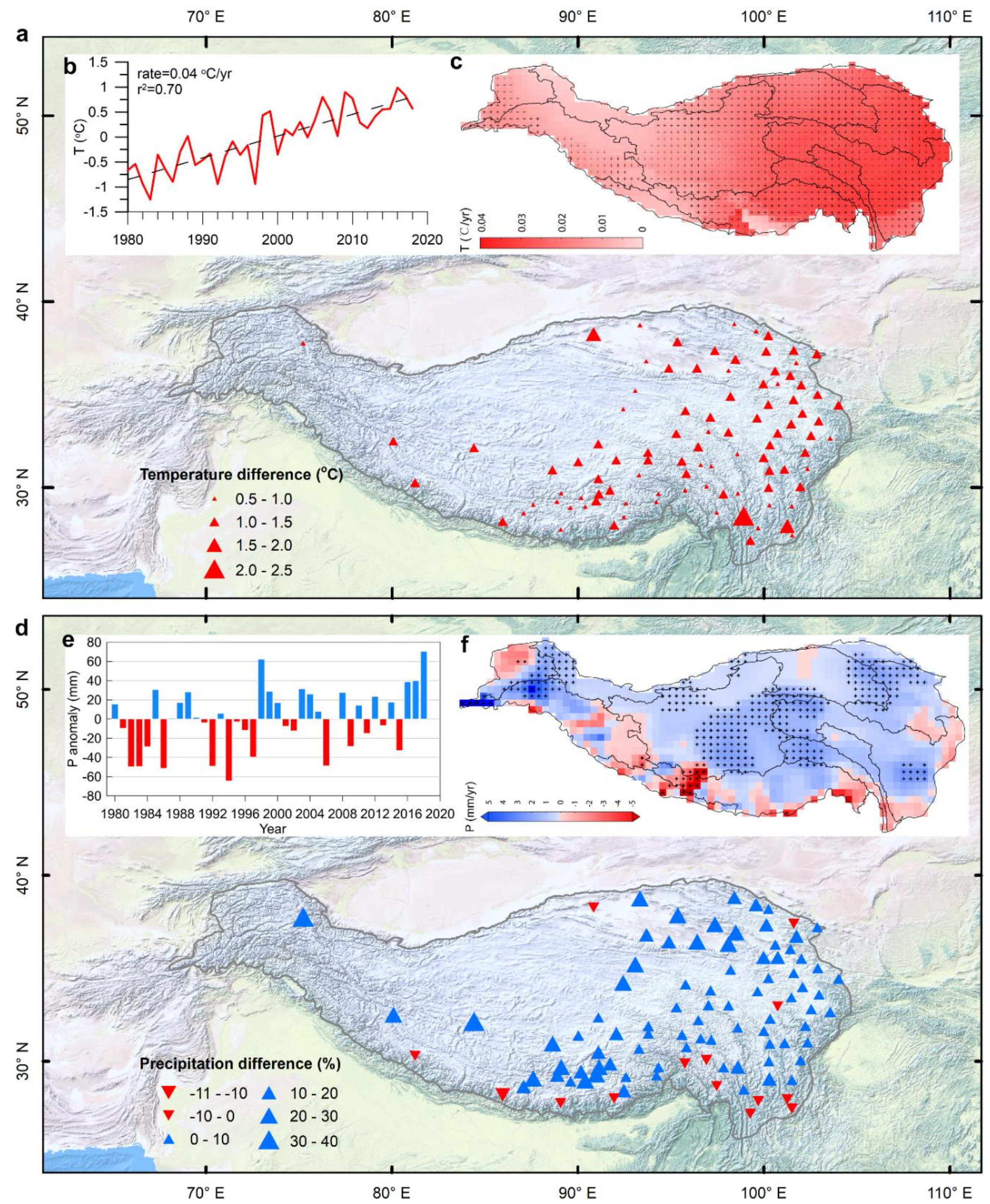

Figure 4. Temperature (T) and precipitation (P) changes. a) T difference between 1998−2018 and 1980−1997 from China Meteorological Administration (CMA) weather station data. b) Annual T anomalies between 1980 and 2018 for the TP. c) Change in T derived from the CRU T data for 1970−2016. d) P difference between 1998−2018 and 1980−1997 from CMA weather station data. e) Anomaly of annual P averaged over all stations for 1980−2018. f) Change in P derived from GPCC data for 1970−2016. The "+" indicates pixels with significant linear trends at a 95% confidence level.

3. Data and methods

3.1 Landsat mission for lake mapping

The Landsat satellite missions, jointly managed by NASA and the U.S. Geological Survey, have been widely used for water body mapping, owing to the long period of data availability (1972−present), coupled with a relatively high spatial resolution, 79 m for MSS (Multispectral Scanner) and 30 m for TM (Thematic Mapper), ETM+ (Enhanced Thematic Mapper Plus), and OLI (Operational Land Imager) (Pekel et al., 2016; Roy et al., 2014; Wulder et al., 2019). Landsat satellite data released at Level-1TP have precision geo-registration and orthorectification using digital topography. The huge Landsat data archive, and especially its free and open data policy, has advanced our knowledge of Earth's long-term surface water variations. The Landsat missions have provided the most comprehensive lake area observations over the TP (Mao et al., 2018; Song et al., 2013; Zhang et al., 2014b; 2019c) (Table S1). However, daily high proportions of cloud-cover, typically covering ~45% of the TP (Yu et al., 2016), and obscuring the lake surfaces, greatly decrease the number of suitable Landsat images for retrieving lake surface area. It is sometimes difficult to find one image for each year in the optimal season (September−December) with relatively stable lake area as well as a low proportion of cloud cover. The October images are prioritized and searched first. If no suitable images are found, then the data for November, December, and September are examined (Zhang et al., 2017a). An image with a cloud-free lake surface in the optimal season is selected, even though it may have a high cloud-cover fraction for the image as a whole.

Lake delineation from Landsat images usually involves manual digitization (Wan et al., 2016; Zhang et al., 2014b) and automated (or semi-automated) water classification (Bolch et al., 2008; Feyisa et al., 2014; Huggel et al., 2002; Ji et al., 2009; Li and Sheng, 2012; Zhang et al., 2017d; 2019d). This visual interpretation is time-consuming and labor intensive, especially for such a vast area as the TP. However, the method, involving a human-computer interaction interpretation process and detailed examination of the original Landsat images, ensures a high level of quality control for the lake boundaries. Automated water classification with high efficiency is necessary for large-scale lake mapping. Many studies have reported various methods of automatic water classification such as spectral water index, single-band thresholding, thematic classification, and the linear unmixing model (Feyisa et al., 2014; Fisher et al., 2016; Huggel et al., 2002; Ji et al., 2009; McFeeters, 1996; Watson et al., 2018; Xu, 2006; Zhang et al., 2017d). Normalized difference water index (NDWI), the most popular method for separating water from non-water features (McFeeters, 1996), is described by a band ratio as given by Eq. (1):

$$\mathrm{NDWI} = (\rho_{\mathrm{green}} - \rho_{\mathrm{NIR}}) / (\rho_{\mathrm{green}} + \rho_{\mathrm{NIR}}) \quad (1)$$

where ρ_{green} and ρ_{NIR} correspond to band 2 and band 4 for TM and ETM+, or band 3 and band 5 for Landsat 8 OLI. The top-of-atmosphere (TOA) reflectance product converted by radiometric calibration from the digital number (DN) of the original Landsat image is used to calculate NDWI (Li et al., 2013b; McFeeters, 2013). First, a TOA radiometric calibration is performed by using Eq. (2):

$$R_{\lambda} = G_{\lambda} \cdot DN + O_{\lambda} \quad (2)$$

where R_λ is spectral radiance at the sensor's aperture [W/(m^2·sr·μm)], and G_λ and O_λ are calibration coefficients gained from Landsat L1T file metadata. TOA reflectance is then computed from Eq. (3) (Chander et al., 2009; Roy et al., 2010; Yang et al., 2015):

$$\rho_{TOA} = \frac{\pi \cdot R_\lambda \cdot d^2}{E_\lambda \cdot Cos\theta_s} \tag{3}$$

where

ρ_{TOA}, Planetary TOA reflectance [unitless]

d, Earth−Sun distance [astronomical units]

E_λ, Mean exo-atmospheric solar irradiance [W/(m^2·μm)]

θ_s, Solar zenith angle [degree]

π, 3.1415926 [a mathematical constant].

Mountain shadows detected by slope threshold (Feng et al., 2016) as well as shaded relief (Li and Sheng, 2012) are excluded from NDWI images for further water delineation. The adjustment of the NDWI threshold can improve water classification accuracy (Ji et al., 2009; Li and Sheng, 2012; Xu, 2006). Some studies have proposed a two-step method (i.e. global-local segmentation) to determine the optimal thresholds (Li and Sheng, 2012; Luo et al., 2009; Sheng et al., 2016). First, a relatively small threshold, usually close to zero, based on previous experience of manual calculation or experiments in selected regions, is used to roughly separate water and non-water features (Li and Sheng, 2012; Zhang et al., 2017a). This initial threshold is not critical as an expanded buffer will be used. Each water body unit is detected and labeled in this step. Second, an outside buffer zone is outlined for each identified water body. An appropriate threshold is then selected for each water body by a nonparametric and unsupervised Otsu method (Otsu, 1979; Zhang et al., 2017d). Water bodies are then successfully separated from other land-cover components. Other water indices, such as the modified NDWI (i.e., MNDWI) (Xu, 2006) and the Automated Water Extraction Index (AWEI) (Feyisa et al., 2014), have also been developed for automatic water classification, but an evaluation of lake-area mapping methods shows that NDWI has a relatively better performance for large-scale water mapping on the TP (Zhang et al., 2017a).

Misclassification of water bodies often occurs, as water turbidity, salt pan, presence of mountain/cloud shadows, and snow/ice can all complicate spectral reflectance (Sheng et al., 2016). In addition, other water body types, such as rivers, reservoirs, and dams, need to be excluded by using available datasets (e.g. Grill et al., 2019; Lehner et al., 2011; Yang and Lu, 2014) and visual examination. Therefore, visual inspection and manual editing, combined with the original Landsat images, are essential for final lake mapping. The Google Earth Engine (GEE), a cloud-based platform, is now a popular tool for water body mapping, as its massive computational capacity can efficiently analyze all archived Landsat images (Gorelick et al., 2017; Pekel et al., 2016). However, a visual examination of global-scale water body products for fine lake classification is difficult, if not impossible. Therefore, a direct application of water bodies produced by the

GEE could result in a large uncertainty in the estimation of lake area (Feng et al., 2019; Zhang et al., 2020b).

Landsat data has irreplaceable advantages for long-term lake observation, but cloud contamination limits its use for seasonal lake mapping. Lake levels from satellite radar altimetry data (Crétaux et al., 2011) or in-situ measurements (Lei et al., 2014) can reveal seasonal characteristics. However, the number of lakes with such available data is small: ~100 out of a total of ~1400 lakes (> 1 km^2) (Zhang et al., 2019c). Sentinel-1 SAR data can be used to detect seasonal cycles of lake area (Miles et al., 2017; Strozzi et al., 2012; Wangchuk et al., 2019; Zhang et al., 2020c), but these data have only been available since 2014. The daily and 8-day MODIS data are also used for water classification maps (Ji et al., 2018; Khandelwal et al., 2017; Pham-Duc et al., 2020), but although the poor spatial resolution (250 or 500 m) is suitable for monitoring dramatic inundation changes such as reservoirs or dams (Gao et al., 2012; Khandelwal et al., 2017), it is not suitable for lakes with small area variations, which is the case for most lakes on the TP (Zhang et al., 2019c). However, the combination of multi-sensor remote sensing data can improve the spatial-temporal resolution of lake observations (Li et al., 2013a; Yamazaki et al., 2015; Yao et al., 2019).

3.2 Monitoring lake level and volume changes

Satellite altimetry missions such as ICESat/ICESat-2, TOPEX/ POSEIDON, Geosat Follow-on, ERS-2, Jason-1/2/3, Envisat, SARAL/Altika, and Cryosat-2 have retrieved lake surface elevation since 1992 (Crétaux et al., 2011; 2016; Jiang et al., 2017a; Markus et al., 2017; Phan et al., 2012; Schutz et al., 2005). These radar and laser altimetry missions are able to monitor lake level elevation and lake level changes with high precision (Bhang et al., 2007; Zhang et al., 2011c; 2019b). The low-resolution radar altimeter has a pulse-limited footprint of a few km in diameter, while the SAR radar altimeter has a finer along-track resolution of ~300 m (Jiang et al., 2017b). In comparison, laser altimetry, for example, ICESat has a smaller footprint diameter of ~70 m. The performance (accuracy and precision) of laser altimetry missions (< 10 cm bias) is better than radar altimetry (decimeter level) (Crétaux et al., 2009; 2011; Zhang et al., 2011c; 2011b). Here, the water levels for 25 lakes with continuous observations derived from radar altimetry between ~1992 and 2018 have been obtained from Hydroweb (http://hydroweb.theia-land.fr/hydroweb) (Crétaux et al., 2011). ICESat/GLA14 laser altimetry data obtained from NASA's National Snow & Ice Data Center (https://nsidc.org/data/icesat) between 2003 and 2009, are also used to monitor lake level changes (Phan et al., 2012; Song et al., 2013; Zhang et al., 2011c; 2013b). The ICESat footprints over water surfaces are selected by using lake boundaries determined from Landsat images. The mean elevation of footprints of a track passing over a lake after outliers have been removed is taken as the lake surface elevation for the time (day). A total of 132 lakes have ICESat data available for a period of longer than 4 years (Zhang et al., 2017c).

ICESat-2 altimetry data have been available since 2018 (https://nsidc.org/data/icesat-2) (Jasinski et al., 2019). The ICESat-2 mission doubles the number of lakes on the TP with altimetry data (236) relative to ICESat (132) (Zhang et al., 2019b). Moreover, ICESat-2 has a better performance, with a precision of ~2 cm when compared with gauge measurements in 2018, and has great potential for monitoring lake level changes.

Lake water volume (storage) gain or loss (ΔV) can be estimated from Eq. (4) by combining lake area and level changes (Taube, 2000):

$$\Delta V = \frac{1}{3}(H_2 - H_1)\times(A_1 + A_2 + \sqrt{A_1 \times A_2}) \qquad (4)$$

where H_1 and H_2 are lake levels in two consecutive stages, and A_1 and A_2 are the corresponding areas.

In this study, water storage changes between the 1970s and 2018 are estimated for lakes with available altimetry data. Lake volume can be directly measured using the Multiple Altimeter Beam Experiment Lidar (MABEL) data, a technology demonstrator for the ICESat-2 mission (Li et al., 2019a; Ma et al., 2019b; McGill et al., 2013). However, this method is limited to lakes shallower than ~5 m (Ma et al., 2019b), and is not suitable for most lakes on the TP which are usually deeper than 20 m (Ma et al., 2014; Qiao et al., 2019a; Wang et al., 2009).

3.3 Estimate of water storage change from GRACE data

The twin co-orbiting NASA/DLR GRACE (Gravity Recovery And Climate Experiment) satellite mission was launched on 17 March 2002. GRACE measures monthly spatiotemporal changes in Earth's gravity field, which can be caused by changes in mass transports of hydrology, ice reservoirs, sea level, and geodynamics including earthquakes, at a spatial scale coarser than 333 km, which helps to improve our understanding of the climate system (Tapley et al., 2019). GRACE ended its science mission in October 2017, and the NASA/GFZ GRACE Follow-On mission was launched on 22 May 2018. The total mass change on the TP was investigated using data from the GRACE satellites (Tapley et al., 2004; Yi et al., 2016). Here, the monthly averaged GRACE Gravity Field Products (GSM) (RL06), processed by the University of Texas at Austin Center for Space Research (http://icgem.gfz-potsdam.de/home), are used. The monthly GSM Degree-1 terms (representing geocenter movement) used the solution from Swenson et al. (2008), and the C20 geopotential coefficients (representing the first term describing the Earth's oblateness) was replaced by solutions derived from the analysis of satellite laser ranging data (Cheng et al., 2011). The effect of glacial isostatic adjustment (GIA) was corrected using a forward GIA model. To minimize any correlated error or denoise, the GRACE estimated TWS change was smoothed by a 500 km Gaussian filter (Wahr et al., 1998) and the signal strength was further recovered by a forward modelling method (Yi et al., 2017). The mass balance in the Inner TP was estimated by a multi-basin inversion approach (Yi et al., 2016; Zhang et al., 2017c).

The Inner TP is a large endorheic basin, and contains majority of the lakes on the TP (Figure 3). The mass balance and lake water balance are evaluated for this basin as a whole (Zhang et al., 2017c). As there is only a limited distribution of weather stations (Figure 4), especially in the western TP, and a large uncertainty in the precipitation products derived from reanalysis and remote sensing data (Tong et al., 2014), it is difficult to make a direct estimate of lake water balance from the precipitation contribution. The TWS change in the Inner TP consists of lake water (*L*), glacier (*G*), snow water equivalent (*SWE*), soil moisture (*SM*), permafrost degradation (*PM*), and groundwater storage (*GWS*), as given in Eq. (5) (Zhang et al., 2017c). In particular, GRACE enables inferring of large-scale groundwater storage changes after removing other hydrologic parameters using auxiliary data sets (Feng et al., 2018; Xiang et al., 2016). Furthermore, lake water balance in the whole Inner TP includes glacier/snow melt and permafrost degradation along with net precipitation (i.e. precipitation minus evaporation, ΔP). Therefore, the net precipitation contribution can be indirectly estimated from the lake water balance by using Eq. (6).

$$\Delta GWS = \Delta TWS - (\Delta L + \Delta G + \Delta SWE + \Delta SM + \Delta PM) \quad (5)$$

$$\Delta P = \Delta L - (\Delta G + \Delta SWE + \Delta PM) \quad (6)$$

3.4 Estimate of lake water surface temperature

The response of lakes on the TP to climate variations, is not only manifested as changes in surface water area, level and volume, but also as changes in lake water surface temperature and lake ice phenology. Rapid and highly variable warming of lake surface waters around the globe have been revealed using a synthesis of in situ and satellite (AVHRR, ATSR) measurements (O'Reilly et al., 2015; Sharma et al., 2015; Woolway and Merchant, 2017). MODIS LST has been shown to perform well in the derivation of land surface temperature and for detecting the warming trend with respect to elevation on the TP (Guo et al., 2019a; Pepin et al., 2019; Qin et al., 2009). MODIS LST products, such as the 8-day nighttime product (MOD11A2), with a spatial resolution of 1 km, have also been used to estimate surface temperature changes of lakes on the TP (Wan et al., 2018; Zhang et al., 2014a). This study displays the warming rates of lake surface water, its elevation dependence, and differences with and without cooling from glacier meltwater.

3.5 Estimate of lake ice phenology

Lake ice provides important ecosystem services such as being an indicator of regional climate change, regulation of the hydrological cycle, recreation, and transportation (Brammer et al., 2014; Hori et al., 2018; Kropáček et al., 2013; Wang et al., 2018a). The date of lake ice break-up has been used as a climatic index (Ruosteenoja, 1986). Widespread loss of lake ice has occurred worldwide in the warming world (Hampton et al., 2016; Sharma et al., 2019). Lake winter ice cover can determine summer water surface warming trends (O'Reilly et al., 2015). Lake ice cover is mainly governed by air temperature, lake depth, elevation and shoreline complexity (Sharma et al., 2019). Lake ice phenology, i.e. the timing of freeze-up, break-up and the duration of lake ice cover, provides valuable information on climatic and local conditions (Sharma et al., 2019). Lake ice phenology is usually described by four parameters: freeze-up start, freeze-up end, break-up start, and break-up end dates. The variations of lake ice phenology on the TP have been monitored by MODIS snow cover products (e.g. MOD10A1, MYD10A1) (Cai et al., 2019; Guo et al., 2018; Kropáček et al., 2013; Qiu et al., 2019) and passive microwave remote sensing data (e.g. SMMR/SSMI) (Cai et al., 2017; Che et al., 2009; Ke et al., 2013). In this study, we summarize the freeze-up start and break-up end dates, lake ice cover duration, and their spatial variabilities from MODIS snow cover data used for the whole TP.

3.6 Gridded climatic data sets

To fill the gaps in the spatial coverage of weather station data (Figure 4), especially in the western TP, monthly gridded temperature data from the Climate Research Unit (CRU) (v4.01, 0.5° resolution) (http://www.cru.uea.ac.uk) between 1970 and 2016 were obtained (Harris et al., 2014). The Global Precipitation Climatology Centre (GPCC) has a better performance in detecting the long-term trend of precipitation change over the TP relative to either the Global Precipitation Climatology Project (GPCP) or PERSIANN-CDR products (Yang et al., 2018). The monthly GPCC data (0.5° resolution) (ftp://ftp.cdc.noaa.gov) (Schneider et al., 2014) between 1970 and 2016 was used. In addition, the APHRODITE daily gridded precipitation data set (APHRO_MA V1101, V1101EX_R1, 0.25º resolution) for the period 1970 to 2015 (http://www.chikyu.ac.jp/precip/english) (Yatagai et al., 2012), constructed from the Asia dense network of rain gauges was used for comparison purposes. The APHRODITE product has shown good performance in revealing the precipitation pattern over High Mountain Asia (HMA), and is widely used (Andermann et al., 2011; Lutz et al., 2014). The Global Land Evaporation Amsterdam Model (GLEAM) data (0.25° resolution, https://www.gleam.eu) (Martens et al., 2017) which has a good ability to model land surface actual evapotranspiration (ETa) over the TP (Liu, 2018) was employed. Although the best products have been selected, quantitative calculations of lake basin water gain or loss using these precipitation and ETa products are difficult, if not impossible, due to large uncertainties over the TP (Li et al., 2020a; Ma et al., 2019a; Tong et al., 2014). Annual temperature, precipitation, and ET changes on the TP between 1970 and 2017 are examined, and used only to compare with the spatial pattern of lake surface water changes.

The Atlantic Multidecadal Oscillation (AMO) index (https://www.esrl.noaa.gov/psd), and Niño 3.4 index (https://climatedataguide.ucar.edu/climate-data) are also used to link the long-term trend and inflection points of lake changes with the large-scale atmospheric circulation (Lei et al., 2014; 2019; Zhang et al., 2017b).

4. Lake area, level and volume changes

4.1 Multi-phase lake number and area changes

Between the 1970s and 2018, lake number and area in the TP presented a robust increase but with a variable trend (Zhang et al., 2014b; 2019c). In 1976, the number of lakes (larger than 1 km^2) was 1081 with a total area of $4.01×10^4$ km^2. By 1990, this value had decreased to 1070 ($3.97×10^4$ km^2), and then increased again to 1204 ($4.13×10^4$ km^2) in 2000 (Figure 5). Between 1990 and 2010, the lake number increased slightly to 1236 lakes in 2010, but the area underwent a rapid expansion with a value of $4.74×10^4$ km^2 in 2010 (a 15% increase). Lake number shows a slight decrease from 2010 to 2015, but a rapid recovery in the most recent three years (2016−2018). The lake number increased to 1424 with a total area of $5.03×10^4$ km^2 in 2018. Over the entire period, 1976−2018, the number of lakes (>1 km^2) has increased by 344 (32%) and the area by $1.02×10^4$ km^2 (25.42%). The number increase in most cases is due to lake expansion from less than 1 km^2 to more than 1 km^2. Of course, some new lakes also appeared (Zhang et al., 2014b), but they contribute a small fraction.

The TP has many large lakes. In 2018, there were 178 lakes larger than 50 km^2. The number of lakes in each size category in 1976 and 2018 is shown in Figure 5. The number of lakes and their aggregated area in each size category show an overall positive increase in 2018, relative to 1976, which contrasts clearly with the overall shrinking of lakes on the adjacent Mongolian Plateau (Tao et al., 2015; Zhang et al., 2017b). The lakes are predominantly located in the Inner TP and lake expansions during 1976–2018 also mainly occurred in this endorheic basin (Figure S2).

A representative example of lake expansion is Selin Co. In 1976, it had an area of 1643.37 km^2, smaller than Nam Co (1949.03 km^2), the largest lake in Tibet at that time. In 2001, the area of Selin Co (2006.38 km^2) exceeded Nam Co (1980.98 km^2). In 2018, Selin Co had increased in area by 46.38% relative to 1976, but Nam Co had only expanded in area by 3.25% during the same period.

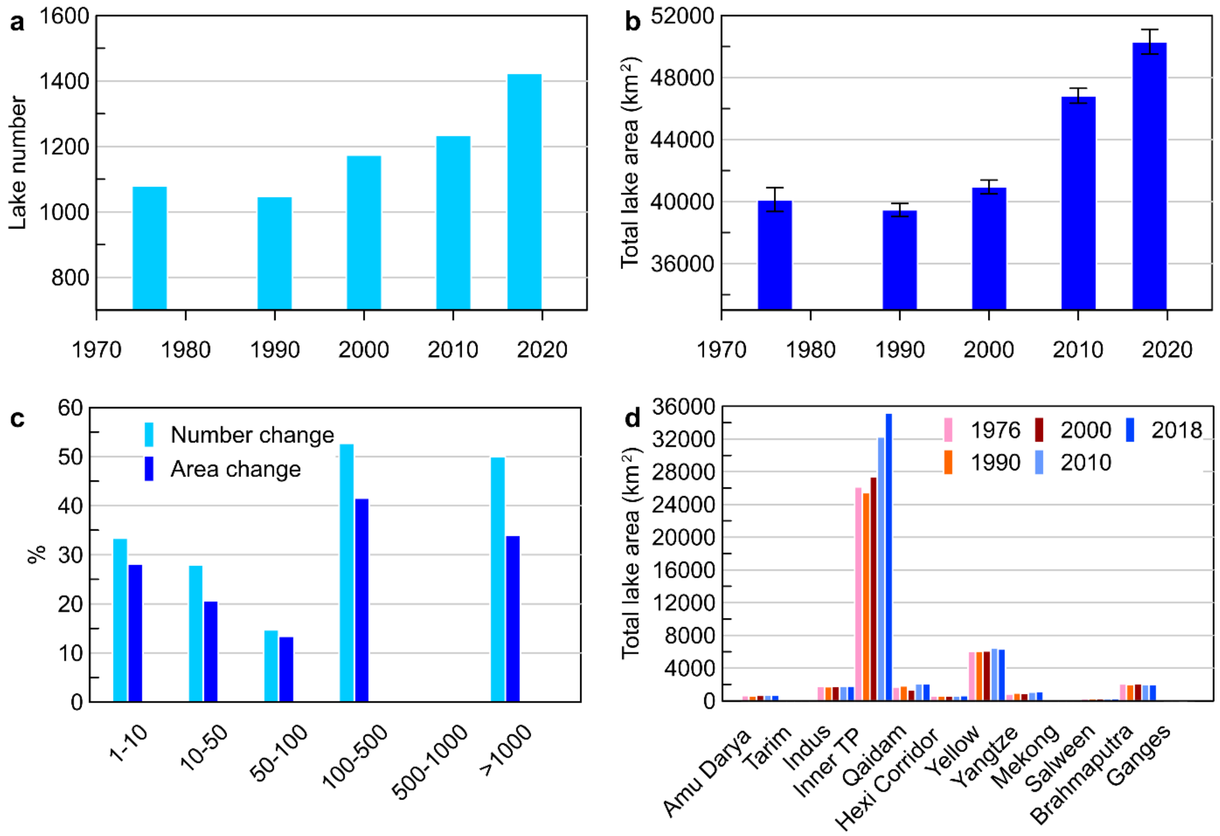

Figure 5. Temporal changes in lake number and area (for lakes > 1 km^2 in area). a) Lake number in 1976, 1990, 2000, 2010 and 2018. The error bar represents the uncertainty of total lake area. b) Total lake area in 1976, 1990, 2000, 2010 and 2018. c) Changes in total lake number and area in different size (km^2) categories in 2018 relative to 1976. d) Total lake area in different lake basins in 1976, 1990, 2000, 2010, and 2018. (Figure 5 adapted from (Zhang et al., 2014b; 2019c))

Spatial differences in lake area changes are also apparent (Figure 6, S2). During the whole period 1976–2018, most lakes expanded in area, especially in the central-north regions (> 32° N). There are a small number of lakes in the southern TP, mainly in the Brahmaputra River basin, such as Yamzho Yumco, Puma Yumco, Paiku Co, Mapam Yumco, La'nga Co, which shrank in area during this period. This suggests a slowing, even reverse pattern of lake expansion from north to south. The difference in the spatial pattern in different periods is large. Based on a clear inflection point detected in 1997/1998 (Zhang et al., 2017b), the lake changes can be divided into two stages. In 1976−1997, almost all lakes, with the exception of a few lakes in the central TP, exhibit area contraction. After 1998, this pattern is reversed, with most lakes showing expansion, especially in the northern TP where the magnitude is generally larger. Many new lakes also appeared after 1998, particularly in the Inner TP.

The regional differences and typical characteristics of lake changes on the TP have also been examined (Lei et al., 2014; Tao et al., 2015; Wan et al., 2014; Yang et al., 2017a; Zhang et al., 2020a). A comparison of lake area between 2005/2006 and 1960s−1980s in Qinghai Province and Tibet Autonomous Region showed a decrease of 7.42% (Wan et al., 2014). The lakes on the endorheic Changtang Plateau continued to expand at a rapid rate of 340.79 km^2/yr during the period 2009−2014, with a 5.57% increase in total area (Yang et al., 2017a). The TP's saline lakes, of which there are 92 larger than 20 km^2 with high salinity, had an area increase of 87.41% in 2010 relative to 1973−1977 (Yan and Zheng, 2015). There is a clear contrast between the lake area increase in the TP, and the shrinkage in Inner Mongolia and the lower reaches of the Yangtze River (Tao et al., 2015; Wang et al., 2017; Zhang et al., 2019d). At the global scale, the expansion of the TP lakes is of a comparable scale to the enormous shrinkage observed in other continents (Pekel et al., 2016).

4.2 Multi-period lake level changes

Lake level changes on the TP have been observed using ICESat laser altimetry data between 2003−2009 (Phan et al., 2012; Song et al., 2013; Zhang et al., 2011c) and radar altimetry missions between 1992 and 2018 (Crétaux et al., 2011; 2016; Jiang et al., 2017a). ICESat altimetry data allows a higher precision in deriving lake water surface elevation than radar altimetry, and enables more lakes to be monitored (Zhang et al., 2011b; 2019b), although it also has clear limitations, such as low temporal resolution (only 2 or 3 collection periods with ~30 days per period, each year), short lifetime (7 years), and the effect of cloud cover on the laser measurements. For 2003−2009, there are about 100 lakes which have more than 4 years of ICESat elevation data (Phan et al., 2012; Song et al., 2013; Zhang et al., 2011c). Lake level changes between 2003 and 2009 show a mean rising rate of ~0.21 m/yr (Zhang et al., 2011c). The mean rate for lakes with increasing water level is 0.26 m/yr, compared to -0.06 m/yr for lakes with decreasing levels. For endorheic lakes, the lake level changes have a mean increasing rate of 0.27 m/yr, compared to 0.12 m/yr for exorheic lakes (Figure S3). In addition, glacier-fed lakes have a slightly higher mean rate of 0.24 m/yr compared with 0.20 m/yr for non-glacier-fed lakes. This observation indirectly implies that increased precipitation could play a dominant role in controlling lake level rising (Song et al., 2014b). A recent study (Treichler et al., 2019; Yao et al., 2018), involving the examination of glacier surface elevation and lake volume changes, also showed that an increase in precipitation has sustained lake growth. The glacier-fed closed lakes show a mean rising rate of 0.26 m/yr, which is greater than the 0.17

m/yr found for non-glacier-fed closed lakes. The differences in the lake level changes could be a result of the unequal numbers of glacier-fed and non-glacier-fed lakes. The spatial pattern of lake level changes is clear, with the majority of lakes with lake level increases situated in the central-northern TP, whilst most lakes with decreasing levels are in the southern TP (Figure 6, S3). Selin Co, the largest lake in Tibet, presents a large water level increase of 0.69 m/yr, but Yamzho Yumco shows a large decline in water level of -0.40 m/yr.

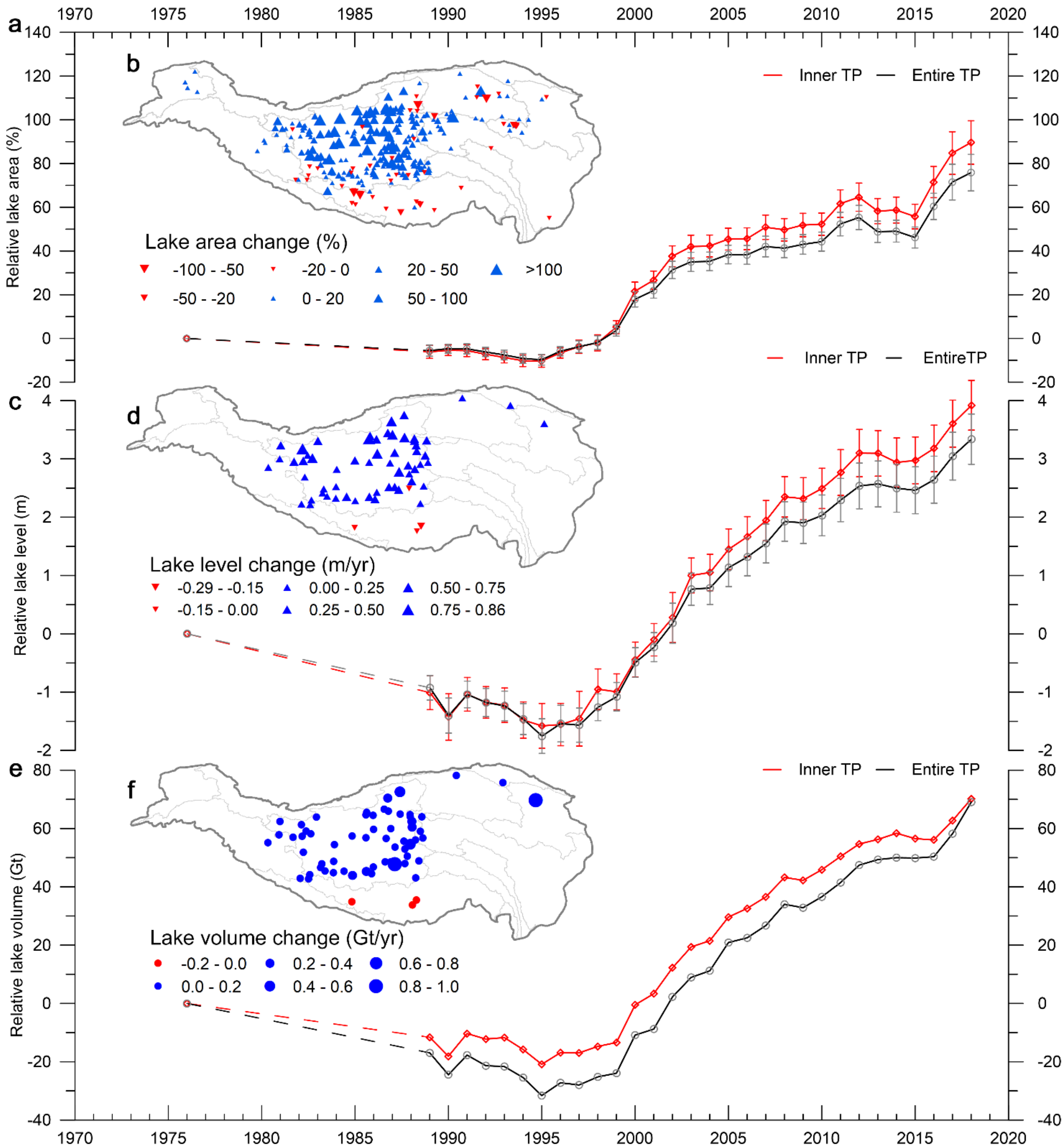

Figure 6. Lake area, level and volume changes for the entire TP (black lines) and Inner TP (red lines). a) Time series of lake area changes (for lakes >10 km^2) relative to 1976. b) Spatial pattern of lake area changes between 1976 and 2018. c) Water level changes relative to 1976 for lakes with available ICESat altimetry data. d) Spatial pattern of lake level change from ICESat/ICESat-2 between 2003 and

2018. Lake levels outside the ICESat/ICESat-2 altimetry period are reconstructed based on the correlation between lake level and area. The error bars indicate the standard error of relative lake area/level change in each year for the lakes used. e) Estimated lake volume changes combining lake area and level changes relative to 1976. f) Spatial pattern of lake volume change between 2003 and 2018. Data courtesy of (Zhang et al., 2017c; 2019c; 2019b).

The water level derived from radar altimetry data for the 25 largest lakes shows a generally increasing trend (Figure S4). The lakes in the northwestern TP (sub-region I) show a more robust increase. The southwestern TP (sub-region II), which includes La'nga Co and Mapam Yumco, is the only region showing a general water level decline. The water level of La'nga Co is variable, but Mapam Yumco has a continuous drop in level, which may be ascribed to water outflow from Mapam Yumco to the closed La'nga Co. The lakes in the southcentral TP (sub-region III) show an increasing but variable trend. Several lakes, such as Dagze Co and Selin Co, have continuous and rapidly increasing levels. Some lakes, such as Nam Co and Pung Co, maintain a relatively stable level after ~2006. Zhari Namco is generally relatively stable, but has had a sharp increase of ~3 m in the most recent three years. The lakes in the northcentral TP (sub-region IV), with the exception of Xuelian Lake, show a continuous and rapid increase in water level. Eling Lake in the northeast (sub-region V) has a variable increasing trend. Qinghai Lake, the largest salt-lake in the TP, has a continuous and rapid increase after 2004. The heterogeneous patterns of lake level changes may be due to differences in lake basin precipitation, glacier meltwater supply, and topographic controls.

Lake outbursts can induce sudden falls in water level. For example, Zhuonai Lake in the Hoh Xil region of the northeastern TP burst on September 15, 2011. This event resulted in a rapid drop in the water level of Zhuonai Lake, but the lakes downstream such as Kusai Lake and Yanhu Lake show correspondingly rapid increases in water level and area (Liu et al., 2016; 2019b). Yanhu Lake requires special attention, because, with a lake level increase of ~10 m from this event, it is now itself vulnerable to bursting (Liu et al., 2019b; Yao et al., 2016). The Qinghai-Tibet railway and highway are ~10 km from Yanhu Lake, and are under threat from its continuous expansion. In addition, the survival of the Tibetan antelope is at risk from the chain response of these lakes (Pei et al., 2019).

After the failure of the ICESat/GLAS altimetry mission, CryoSat-2 can be used to bridge lake level observations. Of 70 large lakes examined using CryoSat-2 SARIn mode data, 48 lakes with increasing levels were found to have a mean rate of 0.28 m/yr, while the other 22 lakes with decreasing levels had a mean negative rate of -0.10 m/yr (Jiang et al., 2017a). The lakes in the northwestern (NW) region had high rates in both the CryoSat-2 period (2010−2015) and the ICESat period (2003−2009) (Figure S5). The lakes in the north-central region also show rapid increases in water level, but the magnitude is small relative to those in the northwestern region. The lakes in the southwestern region show only small changes in level, with half of the lakes having a falling water level. Most lakes in the central region present an increasing lake level, but again the rates are small. Selin Co is an exception, with an increasing rate of 0.37 m/yr in 2010−2015. The southern lakes show a decreasing trend in 2003−2015. In the northeastern plateau, Hala Lake shows a similar rate of 0.15 m/yr in both 2003−2009 and 2010−2015, and Gyaring Lake has a rising trend of 0.24 m/yr in 2003−2009, but a slight negative tendency of -0.02 m/yr in 2010−2015. ICESat-2 launched in September 2018, providing high precision data and has great potential for deriving lake level changes (Zhang et al., 2019b). It will be an important tool when the data become routinely available.

4.3 Long-term continuous lake area/level, and lake water volume changes

Lake water volume changes are estimated by combining variations in both lake area and level (Crétaux et al., 2016; Zhang et al., 2013a). The long time series of lake area changes indicates that both the whole TP and the Inner TP have a slight lake area contraction in 1976−1995, followed by a continuous increase in 1995−2015, and then a rapid expansion between 2015 and 2018, excluding a slight shrinkage which occurred in 2015 (Figure 6). Lake level changes are extended to the whole period 1976−2018 based on the correlation between lake level and lake area obtained for 2003−2009. The time series of lake level shows a decrease from 1976 to 1995. Between 1995 and 2018, the lake level displays a continuous increase, excluding a slight decrease in 2015, which could be associated with the strong 2015/2016 El Niño event (Lei et al., 2019). The pattern of the lake level time series is well correlated with the lake area change time series. The slight differences may be because the number of lakes with lake area mapping available from Landsat data is greater than the number of lakes with lake level obtained from ICESat altimetry data. The uncertainties in the magnitude of lake area and lake level changes may be due to the number of lakes with available data.

Changes in lake volume show a slight decrease between 1976 and 1995, followed by a continuous increase until 2018 (Figure 6). There is a slight decrease of -2.78 Gt/yr in 1970s−1995, then a rapid increase of 12.53 Gt/yr in 1996−2010, followed by a recent deceleration of 1.46 Gt/yr in 2011−2015 (Zhang et al., 2017c). In the most recent three years (2016−2018), lake volume change presents a recovery. The magnitude of lake volume change is not always consistent with lake area change because of the differences in lakeshore topography and lake size (Qiao et al., 2019b).

Spatial patterns of lake volume changes indicate that the majority of lakes in the northern TP (>32 °N) have positive rates of water storage change (Figure 6, S6). The lakes in the southern TP (<32 °N), such as those in the Brahmaputra River basin, have negative rates of water volume change, although the number of lakes and the magnitude of the rates are small. The total lake water change, calculated using Landsat-based lake area and ICESat-based lake level data, shows a mass loss in 1990 and 2000 relative to the 1970s. However, in 2010, the whole TP and Inner TP have water mass gains of ~90 and ~70 Gt, respectively. Between the 1970s and 2015, the mass increases of lake water were ~110 Gt in the TP and ~90 Gt in the Inner TP (Zhang et al., 2017c). In addition, a rate of lake water storage gain of ~14 Gt/yr between 2003 and 2018 from ICESat and ICESat-2 is observed (Zhang et al., 2019b). ICESat water volume changes for more lakes can be estimated from the SRTM DEM elevation intersection with the lake boundaries. Total lake water volume increased by 2.77 Gt/yr in 1976−2013, with a higher rate of 7.67 Gt/yr in recent decades (2000−2013) (Yang et al., 2017b). The Inner TP, the dominant region for water storage, shows a water mass gain of ~7 Gt/yr in both 2000−2009 (Zhang et al., 2013b) and 2002−2015 (Yao et al., 2018). Lake water load can result in subsidence around a lake. For example, InSAR measurements of Selin Co, the largest lake in Tibet, show that rapid area expansion and water level/volume increase, has induced subsidence of ~5 mm/yr (Doin et al., 2015). Conversely, at Yamzho Yumco in the southern TP, there was a ~9 mm crustal rebound over the period 2003−2010 as lake level declined by ~3 m (Zhao et al., 2016).

4.4 TWS changes

The time series of TWS in the Inner TP derived from GRACE data, shows a robust increase before 2012, with a slight decline in 2013−2015, and a recovery of increase in 2016 (Figure S7). The average rate of change of TWS between 2003 and 2016 is ~6.42 Gt/yr. During the period 2003−2009, the entire TP has a total mass gain of ~16.43 Gt/yr, of which ~8.78 Gt/yr can be attributed to lake water storage increase (Wang et al., 2016). For the inner TP, the corresponding rates are ~11.79 Gt/yr and 7.53 Gt/yr. A multi-basin inversion using the GRACE data reveals a tremendous mass accumulation in the TP of ~12.1 Gt/yr during 2003−2014 (Yi et al., 2016), but there are large spatial variations. While there is significant mass gain in the Inner TP, there is a huge mass loss in the southern TP in areas such as the India River and Brahmaputra River basins. The lakes are the primary receptacle of the TWS increase attributable to excess precipitations during the recent decade over the TP. Most of the decline in groundwater storage in northern India can be explained by the consumption of groundwater for irrigation (Asoka et al., 2017; Rodell et al., 2009), while the decrease of TWS in the southeastern TP has been attributed to both decreased precipitation (Yao et al., 2012) and groundwater pumping (Shamsudduha et al., 2012).

The seasonal variation of TWS change on the TP is remarkable and heterogeneous. In the interior region between 2003 and 2015 in the dry season, September−March, TWS has a decreasing trend, but in the wet season, April−August, it has an increasing trend, which is especially marked in June−August (Figure S7). The southern region, for example the Brahmaputra River basin, is wetter in May−August, with a drier pattern in October−December. The northwestern TP becomes wetter from November to March. The seasonal changes of TWS are modulated by the atmospheric moisture budget and the large-scale atmospheric circulation (Meng et al., 2020).

The basin-wide estimate of mass balance in the Inner TP, based on GRACE data, shows that groundwater storage increased at a rate of 5.01±1.59 Gt/yr, which is slightly less than the lake volume increase of 7.72±0.63 Gt/yr in 2003−2009 (Zhang et al., 2017c). The mass balance in the Inner TP indicates that the lake storage (52%) and groundwater (34%) increases are the dominant components, while soil moisture (1%), snow water equivalent (1%), permafrost (-6%) and glaciers (-7%) only make small contributions (Figure 7). A two-dimensional groundwater-flow model reveals that the groundwater flow in the TP is driven and sustained by the topographic gradient and recharge at high elevations (Ge et al., 2008).

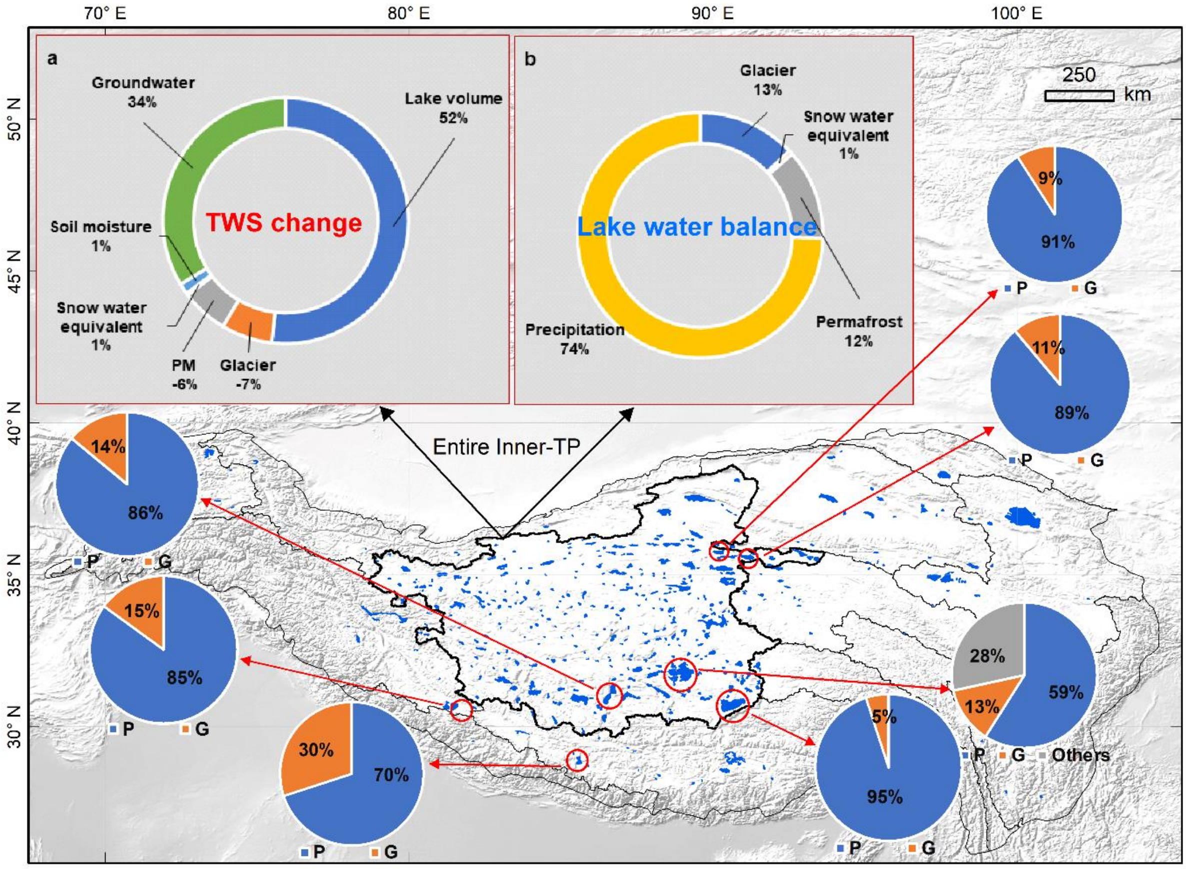

Figure 7. TWS change and lake water balance. a) Changes in TWS from GRACE data, lake water volume, glacier ablation, snow water equivalent, soil moisture, ground ice stored in permafrost (PM), and groundwater storage in the entire Inner-TP. b) Lake water balance estimated from changes in net precipitation, glacier mass, snow water equivalent, and ice stored in permafrost in the entire Inner-TP. In other single lake basins, net precipitation (P) and glacier wastage (G) contributions are provided separately. The composites of lake water balance without further partition are not shown. Data in a−b) from (Zhang et al., 2017c). Individual lake water balances from Table S2.

5. Responses and feedback of lakes to local climate change

5.1 Responses of lakes to climate change

5.1.1 Lake water balance

Evaluations of lake water balance on the TP include both qualitative and quantitative analyses. For the qualitative studies, time series of lake area/level and precipitation are usually compared (Lei et al., 2013; 2014; Zhang et al., 2017b). The results from these studies show that the correlation between lake area, lake level and precipitation (or accumulated precipitation) match well. In addition, comparison of the rates of lake level changes between glacier-fed lakes and non-glacier-fed lakes have been made (Song et al., 2014b; Zhang et al., 2017c). These studies indicate that non-glacier-fed lakes also show high rates of lake level increase, although glacier-fed lakes do show slightly higher rates than non-glacier-fed lakes (Figure S3). This observation could be due to additional water supply from increased glacier meltwater runoff. The gridded CRU temperature product shows that the whole TP became warmer during 1970−2016 (Figure 4). Both gridded GPCC and APHRODITE precipitation products show that the Inner TP is getting wetter, while the southern TP is getting dryer. This contrasting pattern of precipitation change is consistent with lake area/level change. The ETa indicates an overall increase during 1980−2017 (Figure S8). The high-resolution Weather Research and Forecasting (WRF) simulation shows that net precipitation changes over the TP are dominated by precipitation variation (Gao et al., 2015). These studies suggest that precipitation can plausibly explain the long-term trend of lake evolution and spatial patterns, but the contribution of glaciers is not considered.

The basin-scale and individual lake water balances have been also quantitatively examined (Figure 7). For example, lake water balance was evaluated for the entire Inner-TP, and the results showed that increased precipitation contributed the dominant fraction of lake volume increase (~74%), followed by glacier mass loss (~13%), permafrost degradation (~12%), and snow water equivalent (~1%) between 2003 and 2009 (Zhang et al., 2017c). For 2001−2011, the J2000g hydrological model calculated glacier contributions to the lake volume increases of Tangra Yumco, Mapam Yumco, and Paiku Co of ~14%, ~15%, and ~30%, respectively, but higher contributions (~86%, ~85%, and ~70%) from increased precipitation (Biskop et al., 2016). For Nam Co, during 2001−2011, the glacier contribution calculated by the J2000g hydrological model is ~19% (Biskop et al., 2016), while, for 1972−2015, the lumped lake-watershed model gave a value of ~10% (Li et al., 2017a). In addition, the satellite geodetic method suggests that glacier mass loss during 2003−2009 constituted ~10.5% of Nam Co's volume increase (Li and Lin, 2017). For Selin Co, a Water and Energy Budget-based Distributed Hydrological Model indicates that the glaciers contributed ~13% of the lake volume increase during 2003−2012 (Zhou et al., 2015), while, for 1979−2013, a combination of the Variable Infiltration Capacity (VIC) land surface hydrologic model and the degree-day glacier-melt model, gave a value of ~9% (Tong et al., 2016). Glacier mass loss during 2000−2015, calculated by the geodetic method, accounts for ~9.9% and ~11.1% of lake water storage increase for Lexiewudan Lake and Kekexili Lake, respectively (Zhou et al., 2019). The quantitative evaluation of glacier and precipitation contributions, both for the whole Inner-TP and for 7 lake basins separately, reveals that increased precipitation dominates lake water storage gain compared to contributions from glacier mass loss (Figure 7). The contribution of evaporation to large river basins or lake water balance in the TP has rarely been reported. The effect is small, relative to increased precipitation, whether it suppresses or promotes lake level rise. A Flake-simulated annual evaporation of Nam Co since the late 1990s has indicated an increased trend due to energy-related climate changes (Lazhu et al., 2016). However, a decreasing trend of lake surface evaporation has been also found (Guo et al., 2019b; Ma et al., 2016). For example, decreased evaporation from Nam Co during 1979−2012 is only responsible for ~4% of water level increase (Ma et al., 2016). For the largest lake in Tibet, Selin Co, a significant decreasing trend of lake evaporation during 1972−2010 accelerated lake area expansion, but it contributed only ~14% of the lake storage increase (Guo et al., 2019b). The uncertainties from these studies could be due to the models selected and the physical parameters used.

Permafrost degradation due to increasing active-layer thickness has occurred in the TP, but the observations have mainly been made along the Qinghai-Tibet railroad (Luo et al., 2016; Wu et al., 2014; Yang et al., 2010). Based on regional modeling of the active-layer depth over the TP, a rough estimate of the amount of water released from permafrost degradation can be made (Erkan et al., 2011; Oelke and Zhang, 2007; Xiang et al., 2016). In addition, the contribution of melting ground ice to the surface water stream in the source area of the Yellow River, in the northeast TP, has been estimated at 13.2−16.7% by hydrological separation from a stable isotopic method (Yang et al., 2019). Overall, the ground ice melt due to permafrost degradation is still poorly known.

The different study periods, models selected, and input data all result in uncertainties in the various quantitative estimates. In addition, lakes with model-based assessment represent only a small fraction of the more than 100 lakes larger than 100 km^2 in the TP.

5.1.2 Lake water surface temperature changes

Lake water surface temperature is strongly related to regional air and land temperatures, and is a useful indicator of climate change (Adrian et al., 2009). Lake surface waters around the globe reveal rapid and highly variable warming (O'Reilly et al., 2015; Woolway and Merchant, 2017). The water surface temperature of lakes in the TP obtained from a MODIS/Terra 8-day land surface temperature (nighttime) product (MOD11A2), over the period 2001–2012, showed an average warming rate of 0.012 ± 0.033 °C/yr (Zhang et al., 2014a). Of the 52 lakes examined, most (31 lakes, 60%) showed a mean warming rate of 0.055 ± 0.033°C/yr. The other 21 lakes (40%), mainly located at elevations higher than 4200 m a.l.s, had a mean cooling rate of -0.053± 0.038 °C/yr. The majority of lakes in the northern Inner-TP (>33 °N) have a high cooling rate. However, the main lakes in the southern TP (<33 °N) are warming (Figure 8). The altitudinal dependency of lakes with a warming rate shows an increase between 2200 and 4550 m a.s.l., followed by a decrease between 4550 and 4800 m a.s.l., with a relatively stable rate above 4800 m a.s.l (Figure S9). Correspondingly, lakes with a cooling rate have a similar pattern of altitudinal dependency. The patterns of altitudinal dependency of lake water surface temperature are consistent with rates of air temperature and land surface temperature obtained from nearby weather stations (Zhang et al., 2014a).

The reasons behind lake water surface temperature differences and changes may be linked to lake level and lake ice changes. Lake water temperature changes are negatively related to water level changes, especially for freshwater lakes. The water inputs to lakes from precipitation and glacier/snow melt runoff typically have a lower temperature than the lake water, which can modulate lake temperature. For instance, non-glacier-fed lakes have a mean warming rate of 0.038 °C/yr, much higher than the 0.004 °C/yr for glacier-fed lakes (Figure 8), which is the result of cold-water input from glacier melting. In addition, lake water surface temperature changes are highly negatively correlated with lake ice duration (Kropáček et al., 2013; Zhang et al., 2014a). This correlation suggests that a higher lake water temperature shortens lake ice duration, modifying lake ecosystem structure and function. In turn, the decreased lake ice cover can lead to lakes warming faster. The increased lake temperature could be the result of higher air and land surface temperatures warming the lakes by conduction. Higher air temperatures can heat the lake water surface, or accelerate glacier melting in the lake basin, although the latter process has a cooling effect on lakes.

The estimation of lake water temperature can be extended to the early 1980s by using Advanced Very High-Resolution Radiometer (AVHRR) data (Liu et al., 2019a). Examination of long-term trends of surface water temperature, and data from more lakes are required to help understand lake changes in response to the warming climate.

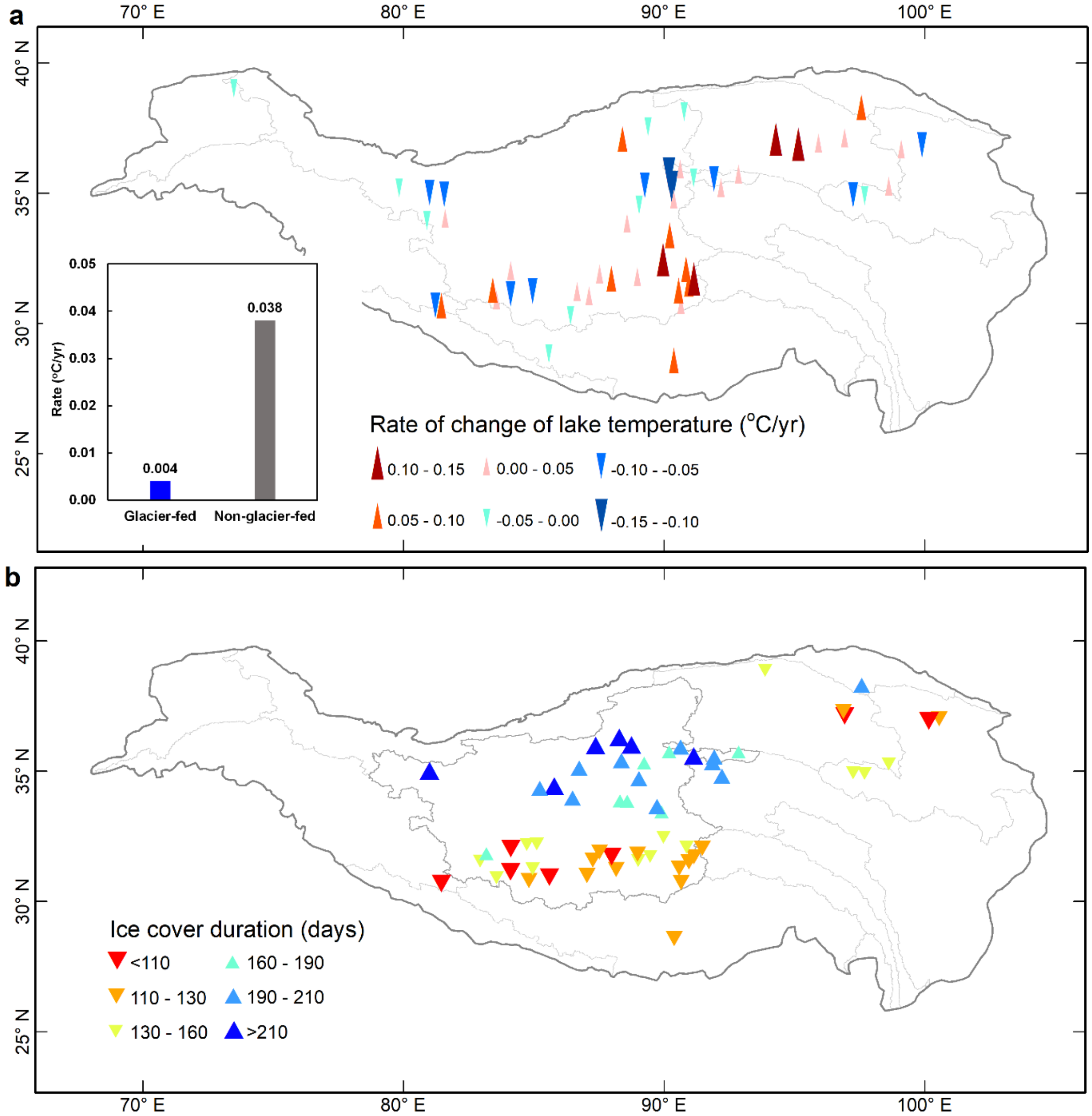

Figure 8. Changes in lake water surface temperature and lake ice cover duration. a) Spatial pattern of lake water temperature changes. Inset shows the mean rates for glacier-fed and non-glacier-fed lakes. b) Spatial pattern of mean lake ice cover duration. Data courtesy of (Zhang et al., 2014a) and (Cai et al., 2019).

5.1.3 Lake ice phenology change

The MODIS snow product provides ice phenology observations for more lakes on the TP than do in-situ measurements (only Qinghai Lake has a long-term in-situ record) (Cai et al., 2019; Guo et al., 2018; Kropáček et al., 2013). Lakes on the TP start to freeze-up in late October and break-up in late March, with the beginning of the ice cover period in mid-January and the end in early July (Cai et al., 2019). For the majority of lakes (69%, 40 out of the 58 lakes with available data), ice cover duration between 2000 and 2017 became shorter at a rate of 0.8 day/yr. For the remaining 18 lakes (31%), ice cover duration increased at a rate of 1.11 day/yr (Cai et al., 2019). The lakes in the northern Inner-TP (>33 ^{o}N) have earlier freeze-up dates and later break-up dates (i.e. a longer ice cover duration) than those in the southern TP (<33 ^{o}N) (Figure 8, S10). This could be due to cooling in the north-central region in comparison to warming in the south-central region in the winter and spring seasons (Guo et al., 2020). It is also consistent with surface cooling of the north-central lakes against surface warming of the south-central lakes (Figure 8a). In addition, the dilution caused by the fast expansion of the north-central lakes (Zhang et al., 2019c) can also result in an earlier freeze-up start date.

Lake ice phenology on the TP is related to climatic conditions, geographical location, and physico-chemical characteristics (Cai et al., 2019). A recent study shows that the lake ice characteristics over the southern TP are the result of the positive NAO-induced atmospheric circulation anomalies (Liu et al., 2019c). Lake ice phenology can also be observed using satellite microwave remote sensing data, such as AMSR-E and AMSR-2 giving a higher temporal resolution but coarse spatial resolution. In the future, it should be possible to extend lake ice phenology observation on the TP back to the early 1980s by using AVHRR sensors (Latifovic and Pouliot, 2007; Weber et al., 2016).

5.2 Feedback of lakes to climate change

The key response of hydrological variables such as lake number, area, level and volume to the effects of climate changes on the lakes have been identified. In this section, the feedbacks of the TP's lakes to climate change are illustrated. The TP's lakes cool the local near-surface air temperature and enhance the mesoscale (over lake surface and surrounding areas) precipitation in summer (Wu et al., 2019; Zhu et al., 2018). These lakes also change regional-scale circulations by weakening the sensible heat flux and strengthening the latent heat flux (Zhu et al., 2018). Such seasonal cooling/heating effects result in the spatial differences of precipitation observed in the Nam Co basin (Dai et al., 2017). In addition, the Weather Research and Forecasting (WRF) simulation shows that Nam Co generates a significant increase (up to 70%) in downwind precipitation in some extreme events, such as the snowstorm on 24 October 2006 (Dai et al., 2018). The cooling effects of Nam Co delay the establishment time of the convective boundary layer (Lv et al., 2008). The expansion of the TP's lakes can affect evaporation by increasing surface water extent. However, the coarse spatial resolution of global terrestrial ET products (1 km or coarser) and large uncertainties in retrieving water surface evaporation (Friedrich et al., 2018; Wang et al., 2018a) are not suitable for estimating evaporative flux change from the areal expansion or shrinkage of individual lakes on the TP. Some studies have indicated that the littoral zones of lakes on the TP are important sources of greenhouse gases (CO_2, CH_4, N_2O) due to their high salinity and pH (e.g. Yan et al., 2018). Broader studies are needed to better understand the effects of lake expansion on altering the regional climate and ecosystems.

6. Response of lake areas to large-scale atmospheric circulation and driving mechanism

6.1 Temporal variability

The TP has become warmer and wetter, especially since the 1990s, and this trend is consistent with the observed trends of lake surface water changes. Variations in the water cycle on the TP may have been driven by changes in the large-scale atmospheric circulation. An inflection point in the trend of lake area changes has been identified in 1997/1998. There is continuous lake area expansion after this point (Zhang et al., 2017b; 2019c). The change in the trend in 1997/1998 is driven by intensified local convection and large scale atmospheric circulation anomalies in response to climate warming (Zhang et al., 2017b). Warming and moistening since 1998 has created a more unstable atmosphere, triggering more deep convection and hence more precipitation (Yang et al., 2012).

Overall, the enhanced hemispheric thermal contrast and Atlantic Multidecadal Oscillation (AMO) have resulted in an intensified Northern Hemisphere summer monsoon (Figure 9) (Wang et al., 2013). A half-century of atmospheric water vapor content, precipitation, and surface temperature data show that the atmospheric moisture supply to the TP has an increasing trend under global warming (Xu et al., 2008), with a clear positive shift of water vapor content occurring around 1997/1998 (Lu et al., 2015). A recent study by Li et al. (2020b) shows that the significantly increased atmospheric transport of water from the Indian Ocean, especially from the western and southern boundaries in summer, was the main cause of the increased precipitation over the Inner TP during 1979−2015.

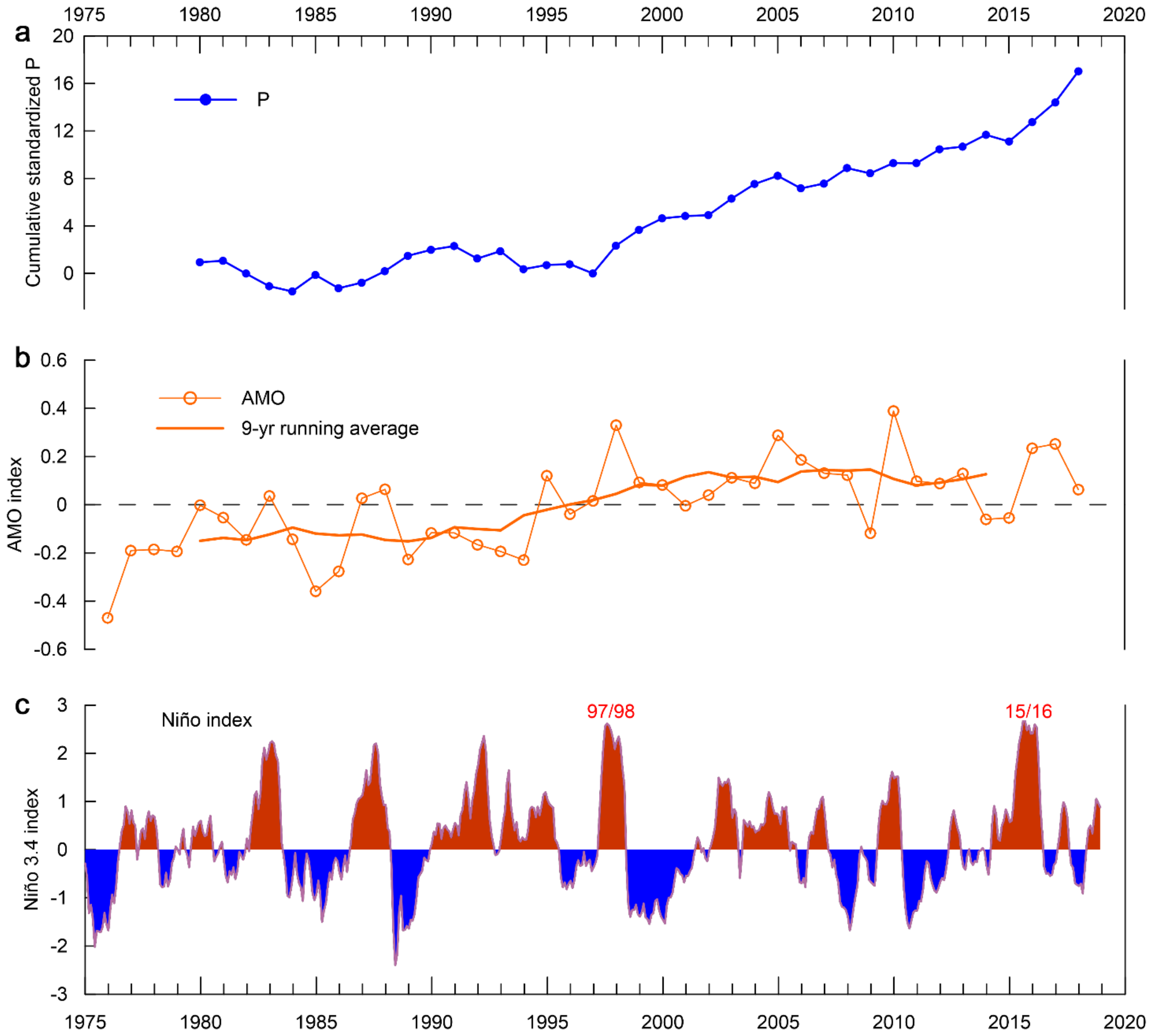

Figure 9. Precipitation and large-scale atmospheric circulation indices on the TP. a) Cumulative standardized precipitation (P) from CMA stations. b) Mean annual Atlantic Multidecadal Oscillation (AMO) from March to May with a 9-yr running average. c) Niño 3.4 index shows warm strong EI Niño (red) and strong La Niña (blue).

The decadal wetting over the Inner TP is linked with both the AMO and global warming. The wetting is associated with a change in the westerlies over the TP (Lin et al., 2013) and, on the inter-decadal scale, is significantly correlated with the AMO (Sun and Yang, 2020). Since the mid-1990s, the AMO has been in its positive phase, with a warm sea surface temperature anomaly in the North Atlantic, and this has led, through modulating Silk Road Pattern waves, to the subtropical westerly jet stream at 200 hPa being weakened and shifting northwards; as a result, an anomalous cyclone to the west of the TP and an anomalous anti-cyclone to the northwest of the TP have emerged (Figure 10). The anomalous cyclone to the west of the TP leads to more moisture transport from the Arabian Sea to the southwestern TP, and the anomalous anti-cyclone to the northwest of the TP causes weaker westerly flow over the eastern TP, eventually resulting in enhanced moisture convergence and increased summer precipitation over the western TP. Meanwhile, the near-surface moistening under global warming has created a more unstable atmosphere, triggering more deep convection and hence more precipitation (Yang et al., 2012).

In addition, the inter-variability of the lake water balance over the TP is modulated by large-scale circulation anomalies. An example is the shrinkage in 2015/2016 when several large lakes were observed to have a slight decrease in water levels (Lei et al., 2019). The strong El Niño event at this time caused enhanced air subsidence and decreased precipitation over the TP (Figure 10).

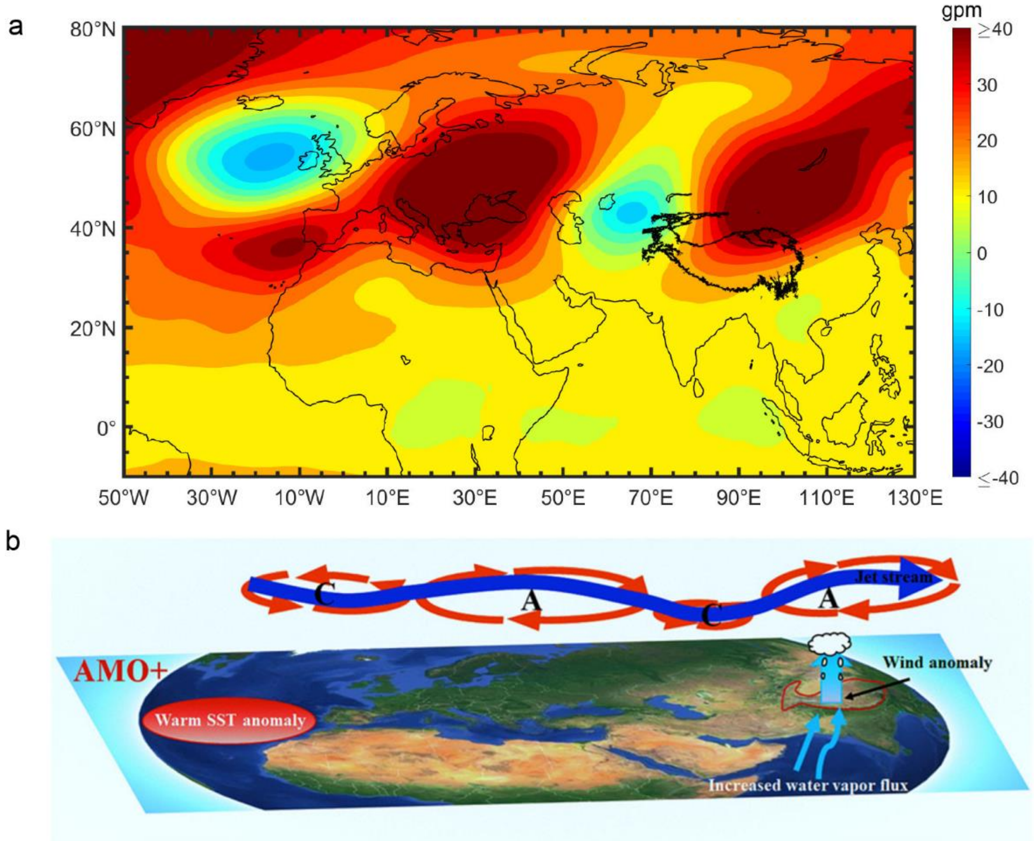

Figure 10. Possible mechanism behind the wetting process in the Inner TP. a) The subtropical westerly jet stream at 200 hPa. b) An anomalous cyclone over the west to the plateau and an anomalous anti-cyclone over the northwest to the plateau. Adapted from (Sun and Yang, 2020).

6.2 Spatial variability

There are clearly contrasting patterns of changes in lake area (level and volume): increasing in the central-northern TP versus decreasing in the southern TP (Lei et al., 2014; Zhang et al., 2014b; 2019b; 2019c), a pattern which is consistent with the observed precipitation differences (Zhang et al., 2019a). The increased precipitation over the northern TP is attributed to the increased moisture transport from the TP and the southeastern regions (Zhang et al., 2019a). However, the decreased precipitation in the southern TP is ascribed to a significant decreasing trend in moisture transport from the northwestern regions.

Nevertheless, it is not clear what drives the decrease in the southern TP. An obvious correlation between the precipitation variability and major atmospheric circulation indices has not been established. Perhaps, both inter-annual and decadal variability have driven the variability of precipitation over the last four decades.

7. Response of lakes to future climate change

Most of the lakes on the TP are situated in the Inner TP, and their response to future climate change has been described by a lake mass balance model (Yang et al., 2018). Assuming the future climate to be even warmer and wetter than its current state, the model predicts that the lake area in the Inner TP will expand continuously from 2015 to 2035 (Figure 11), but at a lower rate than in the period 1995−2015. The predicted future lake levels and volumes, which are validated by existing observations for 1995−2015, show similar patterns to the lake area changes (Zhang et al., 2017c). The projection was made by quantifying future precipitation, but future uncertainties in lake evaporation and glacier mass balance are rarely taken into account in such projections (Yang et al., 2018). Another projection shows that precipitation on the TP will increase by 10.4−11% in 2015−2050 relative to the period 1961−1990 (Chen et al., 2015). Glacier volume will decrease by 9−32% by 2030 under climate scenario RCP4.5, and by 8.7−26.1% under RCP8.5 (Bolch et al., 2019; Giesen and Oerlemans, 2013; Marzeion et al., 2012; Radić et al., 2014). By combining the major contributors to lake water balance from climate (precipitation) and the cryosphere (glaciers), it seems that lake water storage over the TP will increase in the near term (~2035). In addition, as the precipitation over the TP is modulated by AMO, future projections of lake area change may need to consider the impact of both multi-decadal variability and global warming.

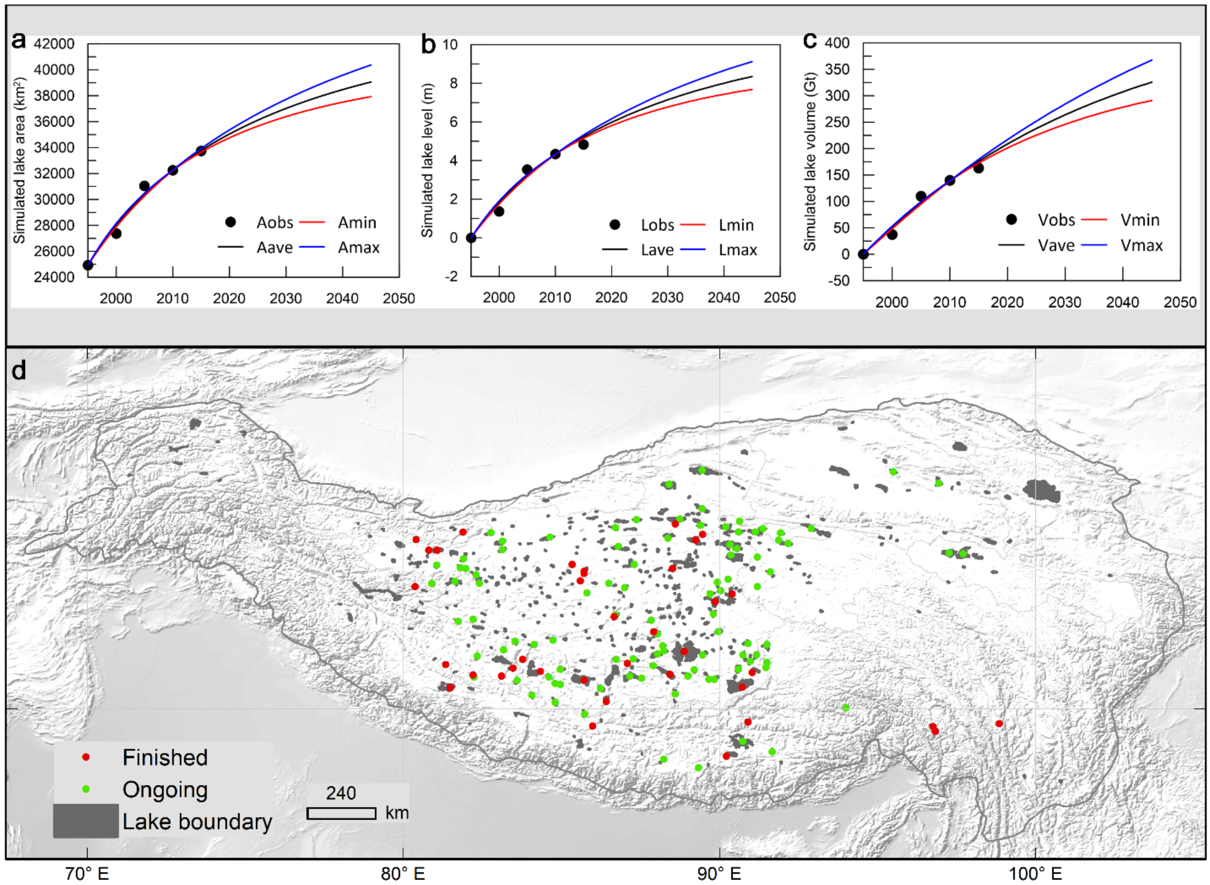

Figure 11. Simulated future lake development and future in-situ lake measurements. a–c) Simulated lake area, level, and water storage development averaged over the Inner TP, under both current climate and reconstructed future climate, relative to 1995. Aobs (lake area), Lobs (lake level) and Vobs (lake volume) are from satellite observations. A, L and V refer to lake area, level and volume respectively, while the subscripts ave, min and max refer to average, minimum and maximum estimates respectively. d) Ongoing and future in-situ lake measurements of bathymetry and water quality (temperature, conductivity, pH, chlorophyll, blue-green algae). Finished (red, counted in early 2019) and ongoing (green) bathymetry and water quality measurements for large lakes (>10 km^2). Data in a–c) from Yang et al. (2018).

8. Conclusions and perspectives

In this review, we examine the detailed characteristics of lake evolution on the TP during the last half-century, and reveal the causes of lake changes and mechanisms. The synthesized spatial patterns of lake hydrological changes, lake water surface temperature change, and lake ice phenology are summarized diagrammatically in Figure 12. The main points are as follows:

(1) The total number and area of lakes on the TP show a drastic but variable increase since the 1970s. The number of lakes (>1 km^2) went up by 32%, from 1,081 in 1976 to 1,424 in 2018. Correspondingly, the total lake area increased by 25.42%, from 4.01×10^4 km^2 in 1976 to 5.03×10^4 km^2 in 2018. This doubled the lake area change (12.26%) of the entire China. Similar to the expansion in area, the mean lake level also showed a rise. Again there were variations in

different periods, for example, ~0.21 m/yr during 2003−2009 and ~0.18 m/yr during 2010−2015. As a result of these changes, the overall lake water storage for the entire TP increased by ~110 Gt from the 1970s to 2015, with most of the gain, ~90 Gt (82%), coming from the Inner TP. The lakes in the northern Inner-TP (>32 ^{o}N) present an increasing expansion, whereas the lakes in the southern TP show continuous shrinkage.

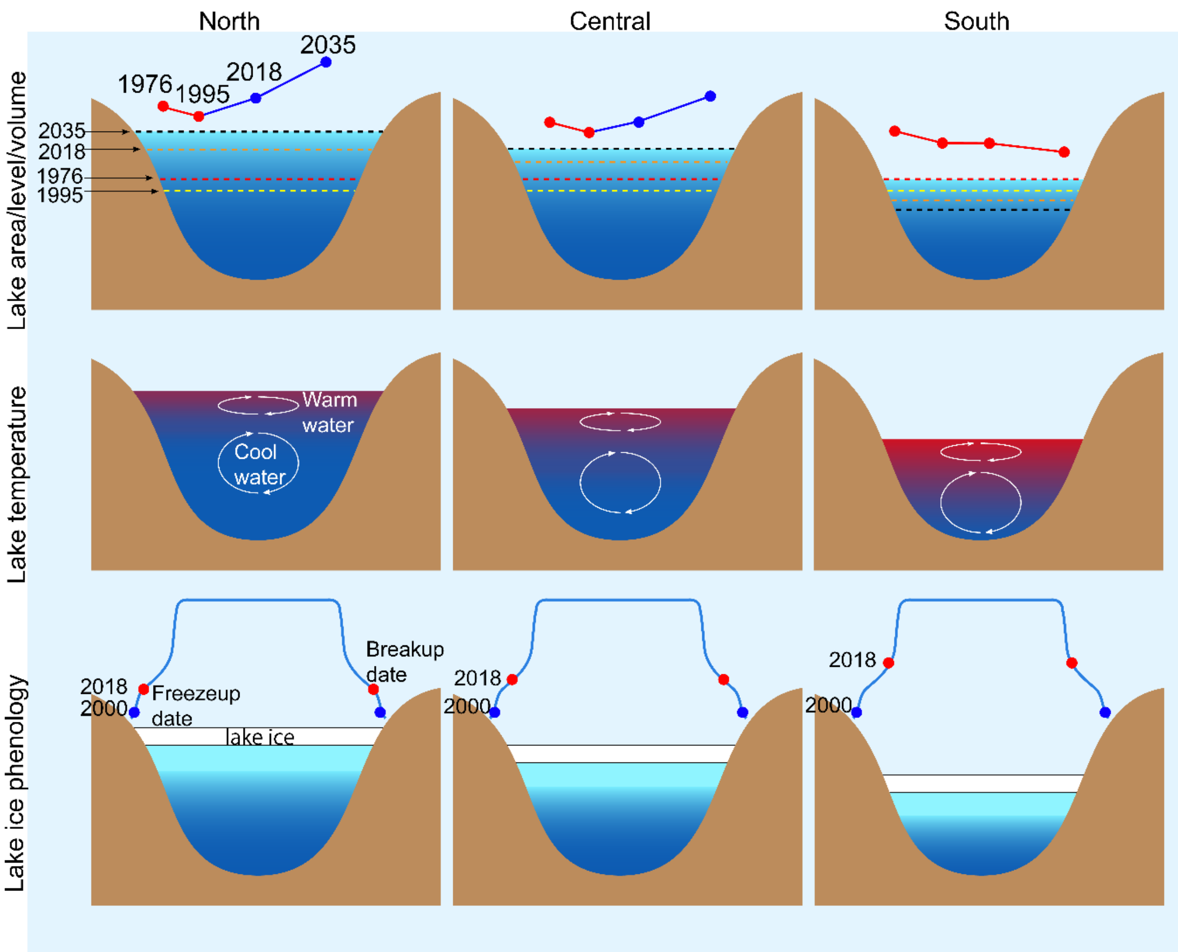

Figure 12. Schematic diagram illustrating spatial patterns of lake area/level/volume, lake water surface temperature, and lake ice cover duration changes on the TP.

(2) The lakes are responding to climate change in many ways, including changes in surface water temperatures and lake ice phenology. Most lakes in the northern Inner-TP (>33 ^{o}N) are cooling, while those in the southern TP are warming. The large differences of lake surface water temperature changes depend on whether the lakes are supplied by glacier meltwater. The changes in lake water surface temperature are negatively correlated with water level variations and lake ice duration. A shorter ice cover duration is observed for the majority of lakes, but this change is heterogenous in space, i.e. there are longer ice cover durations in the northern Inner-TP (>33 ^{o}N) compared with the southern TP.

(3) Enhanced precipitation has been the dominant contributor to increased lake water storage, followed by glacier mass loss and permafrost thawing. The TP has been getting wetter, especially

since the mid-1990s, a trend which is consistent with the interannual trend of lake area expansion. This wetting may be driven by the positive phase (warm anomaly of North Atlantic sea surface) of the AMO. The clear inflection points of lake area/level changes which occurred in 1997/1998 and 2015/2016 can be attributed to strong El Niño events. The spatially contrasting patterns of lake changes may be associated with increased moisture transport from the TP and the southeast regions and decreasing moisture transport from the northwest regions, but this driving mechanism is still under investigation.

(4) The future climate is predicted to be even warmer and wetter, and it is predicted that lake area, level, and volume in the Inner TP will continue to increase in the near term.

In addition, we present some ongoing research programs on the TP and some recommended directions for future research.

- Absolute lake volume estimated by bathymetry measurements. Bathymetry measurements for depths and water storage estimates have always been conducted for some large lakes (Figure 11). In the next five years, with the launch of the Second Tibetan Plateau Scientific Expedition and Research (STEP) program, bathymetry measurements will be made for ~100 large lakes (>10 km^2) (Figure 11). With these measurements, it should be possible to make a comprehensive estimate of absolute lake water storage over the TP.
- Quantitative evaluation of lake water balance. A rough estimate of lake water balance for the Inner TP as a whole has been conducted, but individual lake water balance is only known for a very limited number of lakes such as Nam Co and Selin Co. Especially, few lake evaporation studies have been conducted. With more in-situ measurements made under the STEP program and satellite data from the upcoming SWOT (Surface Water Ocean Topography) mission, for example, it will become possible to estimate quantitatively the drivers (precipitation, evaporation, glacier/snow melting, permafrost degradation) of water storage changes for individual lakes.
- Lake evolution: Past, present, and future. Lake level evolution from the Holocene to the 1970s can be determined by using sediment samples and modern measurement technology such as optically stimulated luminescence (OSL), ^{10}Be, and ^{26}Al exposure dating. Lake level change between the 1970s and 2020 can be derived from lake boundaries obtained from optical satellite images and the intersection of surface water elevation, from DEMs such as SRTM DEM or TanDEM, with the boundaries, enabling the future development (2020−2100) of large lakes under different climate scenarios to be projected.

Acknowledgements

This study was supported by grants from the Second Tibetan Plateau Scientific Expedition and Research (STEP) program (2019QZKK0201), the Strategic Priority Research Program (A) of the Chinese Academy of Sciences (XDA20060201 and XDA19070302), the Natural Science Foundation of China (41871056, 41831177, 21661132003), the National Key R&D Program of China (2018YFB0505005 and 2017YFA0603103-3), and the Field station Alliance Project of the Chinese Academy of Sciences (KFJ-SW-YW038). We would like to thank Catherine M. O'Reilly for her comments at the initial preparation stage of the manuscript and the reviewer for helpful comments to improve the paper.

References

Adrian, R., O'Reilly, C.M., Zagarese, H., Baines, S.B., Hessen, D.O., Keller, W., Livingstone, D.M., Sommaruga, R., Straile, D. and Van Donk, E., 2009. Lakes as sentinels of climate change. Limnology and Oceanography, 54(6): 2283−2297.

Alsdorf, D.E., Rodríguez, E. and Lettenmaier, D.P., 2007. Measuring surface water from space. Rev. Geophys., 45: RG2002.

An, Z., Colman, S.M., Zhou, W., Li, X., Brown, E.T., Jull, A.J.T., Cai, Y., Huang, Y., Lu, X., Chang, H., Song, Y., Sun, Y., Xu, H., Liu, W., Jin, Z., Liu, X., Cheng, P., Liu, Y., Ai, L., Li, X., Liu, X., Yan, L., Shi, Z., Wang, X., Wu, F., Qiang, X., Dong, J., Lu, F. and Xu, X., 2012. Interplay between the Westerlies and Asian monsoon recorded in Lake Qinghai sediments since 32 ka. Sci. Rep., 2: 619.

Andermann, C., Bonnet, S. and Gloaguen, R., 2011. Evaluation of precipitation data sets along the Himalayan front. Geochemistry, Geophysics, Geosystems, 12(7): Q07023.

Asoka, A., Gleeson, T., Wada, Y. and Mishra, V., 2017. Relative contribution of monsoon precipitation and pumping to changes in groundwater storage in India. Nature Geoscience: 109-117.

Barnett, T.P., Adam, J.C. and Lettenmaier, D.P., 2005. Potential impacts of a warming climate on water availability in snow-dominated regions. Nature, 438(7066): 303-309.

Behrangi, A., Gardner, A.S., Reager, J.T. and Fisher, J.B., 2017. Using GRACE to constrain precipitation amount over cold mountainous basins. Geophysical Research Letters, 44(1): 219-227.

Bhang, K.J., Schwartz, F.W. and Braun, A., 2007. Verification of the vertical error in C-band SRTM DEM using ICESat and Landsat-7, Otter Tail County, MN. IEEE Transactions on Geoscience and Remote Sensing, 45(1): 36-44.

Biskop, S., Maussion, F., Krause, P. and Fink, M., 2016. Differences in the water-balance components of four lakes in the southern-central Tibetan Plateau. Hydrol. Earth Syst. Sci., 20(1): 209−225.

Bolch, T., Buchroithner, M., Peters, J., Baessler, M. and Bajracharya, S., 2008. Identification of glacier motion and potentially dangerous glacial lakes in the Mt. Everest region/Nepal using spaceborne imagery. Natural Hazards and Earth System Sciences, 8(6): 1329-1340.

Bolch, T., Shea, J.M., Liu, S., Azam, F.M., Gao, Y., Gruber, S., Immerzeel, W.W., Kulkarni, A., Li, H., Tahir, A.A., Zhang, G. and Zhang, Y., 2019. Status and Change of the Cryosphere in the Extended Hindu Kush Himalaya Region. In: P. Wester, A. Mishra, A. Mukherji and A.B. Shrestha (Editors), The Hindu Kush Himalaya Assessment: Mountains, Climate Change, Sustainability and People. Springer International Publishing, Cham, pp. 209-255.

Brammer, J.R., Samson, J. and Humphries, M.M., 2014. Declining availability of outdoor skating in Canada. Nature Climate Change, 5: 2-4.

Cai, Y., Ke, C., Li, X., Zhang, G., Duan, Z. and Lee, H., 2019. Variations of lake ice phenology on the Tibetan Plateau from 2001 to 2017 based on MODIS Data. Journal of Geophysical Research: Atmospheres, 124(2): 825-843.

Cai, Y., Ke, C.Q. and Duan, Z., 2017. Monitoring ice variations in Qinghai Lake from 1979 to 2016 using passive microwave remote sensing data. Sci Total Environ, 607-608: 120-131.

Chander, G., Markham, B.L. and Helder, D.L., 2009. Summary of current radiometric calibration coefficients for Landsat MSS, TM, ETM+, and EO-1 ALI sensors. Remote Sensing of Environment, 113(5): 893−903.

Che, T., Li, X. and Jin, R., 2009. Monitoring the frozen duration of Qinghai Lake using satellite passive microwave remote sensing low frequency data. Chinese Science Bulletin, 54(13): 2294-2299.

Chen, D., Xu, B., Yao, T., Guo, Z., Cui, P., Chen, F., Zhang, R., Zhang, X., Zhang, Y., Fan, J., Hou, Z. and Zhang, T., 2015. Assessment of past, present and future environmental changes on the Tibetan Plateau. Chinese Science Bulletin, 60(32): 3025−3035.

Cheng, G. and Wu, T., 2007. Responses of permafrost to climate change and their environmental significance, Qinghai-Tibet Plateau. J. Geophys. Res., 112(F2): F02S03.

Cheng, M., Ries, J.C. and Tapley, B.D., 2011. Variations of the Earth's figure axis from satellite laser ranging and GRACE. Journal of Geophysical Research: Solid Earth, 116(B1): B01409.

Crétaux, J.-F., Calmant, S., Romanovski, V., Shabunin, A., Lyard, F., Bergé-Nguyen, M., Cazenave, A., Hernandez, F. and Perosanz, F., 2009. An absolute calibration site for radar altimeters in the continental domain: Lake Issykkul in Central Asia. Journal of Geodesy, 83(8): 723-735.
Crétaux, J.F., Abarca-del-Río, R., Bergé-Nguyen, M., Arsen, A., Drolon, V., Clos, G. and Maisongrande, P., 2016. Lake Volume Monitoring from Space. Surveys in Geophysics, 37(2): 269−305.
Crétaux, J.F., Jelinski, W., Calmant, S., Kouraev, A., Vuglinski, V., Bergé-Nguyen, M., Gennero, M.C., Nino, F., Abarca Del Rio, R., Cazenave, A. and Maisongrande, P., 2011. SOLS: A lake database to monitor in the Near Real Time water level and storage variations from remote sensing data. Advances in Space Research, 47(9): 1497-1507.
Dai, Y., Wang, L., Yao, T., Li, X., Zhu, L. and Zhang, X., 2018. Observed and Simulated Lake Effect Precipitation Over the Tibetan Plateau: An Initial Study at Nam Co Lake. Journal of Geophysical Research: Atmospheres, 123(13): 6746-6759.
Dai, Y., Yao, T., Li, X. and Ping, F., 2017. The impact of lake effects on the temporal and spatial distribution of precipitation in the Nam Co basin, Tibetan Plateau. Quaternary International, 475: 63-69.
Doin, M.-P., Twardzik, C., Ducret, G., Lasserre, C., Guillaso, S. and Jianbao, S., 2015. InSAR measurement of the deformation around Siling Co Lake: Inferences on the lower crust viscosity in central Tibet. Journal of Geophysical Research: Solid Earth, 120(7): 5290-5310.
Erkan, K., Shum, C.K., Wang, L., Guo, J., Jekeli, C., Lee, H., Panero, W.R., Duan, J., Huang, Z. and Wang, H., 2011. Geodetic Constraints on the Qinghai-Tibetan Plateau Present-Day Geophysical Processes. Terrestrial, Atmospheric and Oceanic Sciences, 22(2): 241-253.
Farinotti, D., Huss, M., Fürst, J.J., Landmann, J., Machguth, H., Maussion, F. and Pandit, A., 2019. A consensus estimate for the ice thickness distribution of all glaciers on Earth. Nature Geoscience, 12(3): 168-173.
Feng, M., Sexton, J.O., Channan, S. and Townshend, J.R., 2016. A global, high-resolution (30-m) inland water body dataset for 2000: first results of a topographic–spectral classification algorithm. International Journal of Digital Earth, 9(2): 113-133.
Feng, S., Liu, S., Huang, Z., Jing, L., Zhao, M., Peng, X., Yan, W., Wu, Y., Lv, Y., Smith, A.R., McDonald, M.A., Patil, S.D., Sarkissian, A.J., Shi, Z., Xia, J. and Ogbodo, U.S., 2019. Inland water bodies in China: Features discovered in the long-term satellite data. Proceedings of the National Academy of Sciences, 116(51): 25491-25496.
Feng, W., Shum, C., Zhong, M. and Pan, Y., 2018. Groundwater Storage Changes in China from Satellite Gravity: An Overview. Remote Sensing, 10(5).
Feyisa, G.L., Meilby, H., Fensholt, R. and Proud, S.R., 2014. Automated Water Extraction Index: A new technique for surface water mapping using Landsat imagery. Remote Sensing of Environment, 140: 23−35.
Fisher, A., Flood, N. and Danaher, T., 2016. Comparing Landsat water index methods for automated water classification in eastern Australia. Remote Sensing of Environment, 175: 167−182.
Friedrich, K., Grossman, R.L., Huntington, J., Blanken, P.D., Lenters, J., Holman, K.D., Gochis, D., Livneh, B., Prairie, J., Skeie, E., Healey, N.C., Dahm, K., Pearson, C., Finnessey, T., Hook, S.J. and Kowalski, T., 2018. Reservoir Evaporation in the Western United States: Current Science, Challenges, and Future Needs. Bulletin of the American Meteorological Society, 99(1): 167-187.
Gao, H., Birkett, C. and Lettenmaier, D.P., 2012. Global monitoring of large reservoir storage from satellite remote sensing. Water Resour. Res., 48(9): W09504.
Gao, Y., Leung, L.R., Zhang, Y. and Cuo, L., 2015. Changes in Moisture Flux over the Tibetan Plateau during 1979–2011: Insights from a High-Resolution Simulation. Journal of Climate, 28(10): 4185−4197.
Ge, S., Wu, Q.B., Lu, N., Jiang, G.L. and Ball, L., 2008. Groundwater in the Tibet Plateau, western China. Geophysical Research Letters, 35(18): L18403.
Giesen, R.H. and Oerlemans, J., 2013. Climate-model induced differences in the 21st century global and regional glacier contributions to sea-level rise. Climate Dynamics, 41(11): 3283-3300.
Gorelick, N., Hancher, M., Dixon, M., Ilyushchenko, S., Thau, D. and Moore, R., 2017. Google Earth Engine: Planetary-scale geospatial analysis for everyone. Remote Sensing of Environment, 202: 18-27.
Grill, G., Lehner, B., Thieme, M., Geenen, B., Tickner, D., Antonelli, F., Babu, S., Borrelli, P., Cheng, L., Crochetiere, H., Ehalt Macedo, H., Filgueiras, R., Goichot, M., Higgins, J., Hogan, Z., Lip, B., McClain, M.E., Meng, J., Mulligan, M., Nilsson, C., Olden, J.D., Opperman, J.J., Petry, P., Reidy Liermann, C., Saenz, L., Salinas-Rodriguez, S., Schelle, P., Schmitt, R.J.P., Snider, J., Tan, F., Tockner, K., Valdujo, P.H., van Soesbergen, A. and Zarfl, C., 2019. Mapping the world's free-flowing rivers. Nature, 569(7755): 215-221.
Guo, D., Sun, J., Yang, K., Pepin, N. and Xu, Y., 2019a. Revisiting recent elevation-dependent warming on the Tibetan Plateau using satellite-based datasets. Journal of Geophysical Research: Atmospheres, 124(15): 8511-8521.
Guo, D., Sun, J., Yang, K., Pepin, N., Xu, Y., Xu, Z. and Wang, H., 2020. Satellite data reveal southwestern Tibetan plateau cooling since 2001 due to snow-albedo feedback. International Journal of Climatology, 40(3): 1644-1655.

Guo, L., Wu, Y., Zheng, H., Zhang, B., Li, J., Zhang, F. and Shen, Q., 2018. Uncertainty and Variation of Remotely Sensed Lake Ice Phenology across the Tibetan Plateau. Remote Sensing, 10(10): 1534.
Guo, W., Liu, S., Xu, J., Wu, L., Shangguan, D., Yao, X., Wei, J., Bao, W., Yu, P., Liu, Q. and Jiang, Z., 2015. The second Chinese glacier inventory: data, methods and results. Journal of Glaciology, 61(226): 357−372.
Guo, Y., Zhang, Y., Ma, N., Xu, J. and Zhang, T., 2019b. Long-term changes in evaporation over Siling Co Lake on the Tibetan Plateau and its impact on recent rapid lake expansion. Atmospheric Research, 216: 141-150.
Hampton, S.E., Galloway, A.W., Powers, S.M., Ozersky, T., Woo, K.H., Batt, R.D., Labou, S.G., O'Reilly, C.M., Sharma, S., Lottig, N.R., Stanley, E.H., North, R.L., Stockwell, J.D., Adrian, R., Weyhenmeyer, G.A., Arvola, L., Baulch, H.M., Bertani, I., Bowman, L.L., Jr., Carey, C.C., Catalan, J., Colom-Montero, W., Domine, L.M., Felip, M., Granados, I., Gries, C., Grossart, H.P., Haberman, J., Haldna, M., Hayden, B., Higgins, S.N., Jolley, J.C., Kahilainen, K.K., Kaup, E., Kehoe, M.J., MacIntyre, S., Mackay, A.W., Mariash, H.L., McKay, R.M., Nixdorf, B., Noges, P., Noges, T., Palmer, M., Pierson, D.C., Post, D.M., Pruett, M.J., Rautio, M., Read, J.S., Roberts, S.L., Rucker, J., Sadro, S., Silow, E.A., Smith, D.E., Sterner, R.W., Swann, G.E., Timofeyev, M.A., Toro, M., Twiss, M.R., Vogt, R.J., Watson, S.B., Whiteford, E.J. and Xenopoulos, M.A., 2016. Ecology under lake ice. Ecol Lett, 20(1): 98-111.
Harris, I., Jones, P.D., Osborn, T.J. and Lister, D.H., 2014. Updated high-resolution grids of monthly climatic observations – the CRU TS3.10 Dataset. International Journal of Climatology, 34(3): 623−642.
Hori, Y., Cheng, V.Y.S., Gough, W.A., Jien, J.Y. and Tsuji, L.J.S., 2018. Implications of projected climate change on winter road systems in Ontario’s Far North, Canada. Climatic Change, 148(1): 109-122.
Huang, C., Chen, Y., Zhang, S. and Wu, J., 2018. Detecting, extracting and monitoring surface water from space using optical sensors - a review. Reviews of Geophysics, 56(2): 333-360.
Huggel, C., Kääb, A., Haeberli, W., Teysseire, P. and Paul, F., 2002. Remote sensing based assessment of hazards from glacier lake outbursts: a case study in the Swiss Alps. Canadian Geotechnical Journal, 39(2): 316-330.
Immerzeel, W.W., Beek, L.P.H. and Bierkens, M.F.P., 2010. Climate Change Will Affect the Asian Water Towers. Science, 328(5984): 1382-1385.
Immerzeel, W.W., Lutz, A.F., Andrade, M., Bahl, A., Biemans, H., Bolch, T., Hyde, S., Brumby, S., Davies, B.J., Elmore, A.C., Emmer, A., Feng, M., Fernández, A., Haritashya, U., Kargel, J.S., Koppes, M., Kraaijenbrink, P.D.A., Kulkarni, A.V., Mayewski, P., Nepal, S., Pacheco, P., Painter, T.H., Pellicciotti, F., Rajaram, H., Rupper, S., Sinisalo, A., Shrestha, A.B., Viviroli, D., Wada, Y., Xiao, C., Yao, T. and Baillie, J.E.M., 2020. Importance and vulnerability of the world’s water towers. Nature, 577: 364–369.
Jasinski, M., Stoll, J., Hancock, D., Robbins, J., Nattala, J., Pavelsky, T., Morrison, J., Arp, C., Jones, B. and ICESat-2-Science-Team, 2019. ATLAS/ICESat-2 L3A Inland Water Surface Height, Version 1. [Indicate subset used]. Boulder, Colorado USA. NASA National Snow and Ice Data Center Distributed Active Archive Center.
Ji, L., Gong, P., Wang, J., Shi, J. and Zhu, Z., 2018. Construction of the 500 m resolution daily global surface water change database (2001-2016). Water Resources Research, 54(12): 10270-10292.
Ji, L., Zhang, L. and Wylie, B., 2009. Analysis of Dynamic Thresholds for the Normalized Difference Water Index. Photogrammetric Engineering & Remote Sensing, 75(11): 1307−1317.
Jiang, L., Nielsen, K., Andersen, O.B. and Bauer-Gottwein, P., 2017a. Monitoring recent lake level variations on the Tibetan Plateau using CryoSat-2 SARIn mode data. Journal of Hydrology, 544: 109-124.
Jiang, L., Schneider, R., Andersen, O. and Bauer-Gottwein, P., 2017b. CryoSat-2 Altimetry Applications over Rivers and Lakes. Water, 9(3): 211.
Kang, S.C., Xu, Y.W., You, Q.L., Flugel, W.A., Pepin, N. and Yao, T.D., 2010. Review of climate and cryospheric change in the Tibetan Plateau. Environ. Res. Lett., 5: 015101.
Ke, C.-Q., Tao, A.-Q. and Jin, X., 2013. Variability in the ice phenology of Nam Co Lake in central Tibet from scanning multichannel microwave radiometer and special sensor microwave/imager: 1978 to 2013. Journal of Applied Remote Sensing, 7(1): 073477-073477.
Khandelwal, A., Karpatne, A., Marlier, M.E., Kim, J., Lettenmaier, D.P. and Kumar, V., 2017. An approach for global monitoring of surface water extent variations in reservoirs using MODIS data. Remote Sensing of Environment, 202: 113-128.
Kropáček, J., Maussion, F., Chen, F., Hoerz, S. and Hochschild, V., 2013. Analysis of ice phenology of lakes on the Tibetan Plateau from MODIS data. The Cryosphere, 7(1): 287−301.
Kuang, X. and Jiao, J.J., 2016. Review on climate change on the Tibetan Plateau during the last half century. Journal of Geophysical Research: Atmospheres, 121(8): 3979-4007.
Latifovic, R. and Pouliot, D., 2007. Analysis of climate change impacts on lake ice phenology in Canada using the historical satellite data record. Remote Sensing of Environment, 106(4): 492-507.
Lazhu, Yang, K., Wang, J., Lei, Y., Chen, Y., Zhu, L., Ding, B. and Qin, J., 2016. Quantifying evaporation and its decadal change for Lake Nam Co, Central Tibetan Plateau. Journal of Geophysical Research: Atmospheres: 7578-7591.

Lehner, B., Liermann, C.R., Revenga, C., Vörösmarty, C., Fekete, B., Crouzet, P., Döll, P., Endejan, M., Frenken, K., Magome, J., Nilsson, C., Robertson, J.C., Rödel, R., Sindorf, N. and Wisser, D., 2011. High-resolution mapping of the world's reservoirs and dams for sustainable river-flow management. Frontiers in Ecology and the Environment, 9(9): 494-502.

Lei, Y., Yang, K., Wang, B., Sheng, Y., Bird, B.W., Zhang, G. and Tian, L., 2014. Response of inland lake dynamics over the Tibetan Plateau to climate change. Climatic Change, 125: 281−290.

Lei, Y., Yao, T., Bird, B.W., Yang, K., Zhai, J. and Sheng, Y., 2013. Coherent lake growth on the central Tibetan Plateau since the 1970s: characterization and attribution. Journal of Hydrology, 483: 61−67.

Lei, Y., Zhu, Y., Wang, B., Yao, T., Yang, K., Zhang, X., Zhai, J. and Ma, N., 2019. Extreme lake level changes on the Tibetan Plateau associated with the 2015/2016 El Niño. Geophysical Research Letters, 46(11): 5889-5898.

Li, B., Zhang, J., Yu, Z., Liang, Z., Chen, L. and Acharya, K., 2017a. Climate change driven water budget dynamics of a Tibetan inland lake. Global and Planetary Change, 150: 70-80.

Li, D., Yang, K., Tang, W., Li, X., Zhou, X. and Guo, D., 2020a. Characterizing precipitation in high altitudes of the western Tibetan Plateau with a focus on major glacier areas. International Journal of Climatology: 1-14.

Li, G. and Lin, H., 2017. Recent decadal glacier mass balances over the Western Nyainqentanglha Mountains and the increase in their melting contribution to Nam Co Lake measured by differential Bistatic SAR interferometry. Global and Planetary Change, 149: 177-190.

Li, J., 1999. Studies on the Geomorphological Evolution of the Qinghai Xizang (Tibetan) Plateau and Asian Monsoon. Marine geology & Quaternary geology, 19(1): 1-11.

Li, J. and Sheng, Y., 2012. An automated scheme for glacial lake dynamics mapping using Landsat imagery and digital elevation models: a case study in the Himalayas. International Journal of Remote Sensing, 33(16): 5194−5213.

Li, S., Sun, D., Goldberg, M. and Stefanidis, A., 2013a. Derivation of 30-m-resolution water maps from TERRA/MODIS and SRTM. Remote Sensing of Environment, 134: 417-430.

Li, W., Du, Z., Ling, F., Zhou, D., Wang, H., Gui, Y., Sun, B. and Zhang, X., 2013b. A Comparison of Land Surface Water Mapping Using the Normalized Difference Water Index from TM, ETM+ and ALI. Remote Sensing, 5(11): 5530−5549.

Li, X., Wang, L., Guo, X. and Chen, D., 2017b. Does summer precipitation trend over and around the Tibetan Plateau depend on elevation? International Journal of Climatology, 37: 1278-1284.

Li, Y., Gao, H., Jasinski, M.F., Zhang, S. and Stoll, J.D., 2019a. Deriving High-Resolution Reservoir Bathymetry From ICESat-2 Prototype Photon-Counting Lidar and Landsat Imagery. IEEE Transactions on Geoscience and Remote Sensing, 57(10): 7883-7893.

Li, Y., Su, F., Chen, D. and Tang, Q., 2020b. Atmospheric Water Transport to the Endorheic Tibetan Plateau and Its Effect on the Hydrological Status in the Region. Journal of Geophysical Research: Atmospheres, 124(23): 12864-12881.

Li, Z., Feng, Q., Li, Z., Yuan, R., Gui, J. and Lv, Y., 2019b. Climate background, fact and hydrological effect of multiphase water transformation in cold regions of the Western China: A review. Earth-Science Reviews, 190: 33-57.

Lin, C., Chen, D., Yang, K. and Ou, T., 2018. Impact of model resolution on simulating the water vapor transport through the central Himalayas: implication for models' wet bias over the Tibetan Plateau. Climate Dynamics, 51(9): 3195-3207.

Lin, C., Yang, K., Qin, J. and Fu, R., 2013. Observed Coherent Trends of Surface and Upper-Air Wind Speed over China since 1960. Journal of Climate, 26(9): 2891-2903.

Liu, B., Du, Y.e., Li, L., Feng, Q., Xie, H., Liang, T., Hou, F. and Ren, J., 2016. Outburst Flooding of the Moraine-Dammed Zhuonai Lake on Tibetan Plateau: Causes and Impacts. IEEE Geoscience and Remote Sensing Letters, 13(4): 570-574.

Liu, B., Wan, W., Xie, H., Li, H., Zhu, S., Zhang, G., Wen, L. and Hong, Y., 2019a. A long-term dataset of lake surface water temperature over the Tibetan Plateau derived from AVHRR 1981–2015. Scientific Data, 6(1): 48.

Liu, W., 2018. Evaluating remotely sensed monthly evapotranspiration against water balance estimates at basin scale in the Tibetan Plateau. Hydrology Research, 49(6): 1977-1990.

Liu, W., Xie, C., Zhao, L., Wu, T., Wang, W., Zhang, Y., Yang, G., Zhu, X. and Yue, G., 2019b. Dynamic changes in lakes in the Hoh Xil region before and after the 2011 outburst of Zonag Lake. Journal of Mountain Science, 16(5): 1098-1110.

Liu, X., Cheng, Z., Yan, L. and Yin, Z.-Y., 2009. Elevation dependency of recent and future minimum surface air temperature trends in the Tibetan Plateau and its surroundings. Global and Planetary Change, 68(3): 164-174.

Liu, X.D. and Chen, B.D., 2000. Climatic warming in the Tibetan Plateau during recent decades. International Journal of Climatology, 20(14): 1729-1742.

Liu, Y., Chen, H., Wang, H. and Qiu, Y., 2019c. The impact of the NAO on the delayed break-up date of lake ice over the southern Tibetan Plateau. Journal of Climate, 31: 9073-9086.
Liu, Y., Lu, M., Yang, H., Duan, A., He, B., Yang, S. and Wu, G., 2020. Land–atmosphere–ocean coupling associated with the Tibetan Plateau and its climate impacts. National Science Review, 7(3): 534-552.
Lu, N., Trenberth, K.E., Qin, J., Yang, K. and Yao, L., 2015. Detecting Long-Term Trends in Precipitable Water over the Tibetan Plateau by Synthesis of Station and MODIS Observations. Journal of Climate, 28(4): 1707−1722.
Luo, D., Wu, Q., Jin, H., Marchenko, S.S., Lü, L. and Gao, S., 2016. Recent changes in the active layer thickness across the northern hemisphere. Environmental Earth Sciences, 75: 555.
Luo, J., Sheng, Y. and Shen, Z., 2009. Automatic and high-precise extraction for water information from multispectral images with the step-by-step iterative transformation mechanism. Journal of Remote Sensing, 13(4): 610−615.
Lutz, A.F., Immerzeel, W.W., Shrestha, A.B. and Bierkens, M.F.P., 2014. Consistent increase in High Asia's runoff due to increasing glacier melt and precipitation. Nature Climate Change, 4(7): 587-592.
Lv, Y., Ma, Y., Li, M. and Yang, X., 2008. Numerical simulation of typical atmospheric boundary layer characteristics over Lake Nam Co region, Tibetan Plateau in summer. Plateau Meteorology, 27: 733-740.
Ma, N., Szilagyi, J., Niu, G.-Y., Zhang, Y., Zhang, T., Wang, B. and Wu, Y., 2016. Evaporation variability of Nam Co Lake in the Tibetan Plateau and its role in recent rapid lake expansion. Journal of Hydrology, 537: 27-35.
Ma, N., Szilagyi, J., Zhang, Y. and Liu, W., 2019a. Complementary-Relationship-Based Modeling of Terrestrial Evapotranspiration Across China During 1982–2012: Validations and Spatiotemporal Analyses. Journal of Geophysical Research: Atmospheres, 124(8): 4326-4351.
Ma, Q., Zhu, L., Lü, X., Guo, Y., Ju, J., Wang, J., Wang, Y. and Tang, L., 2014. Pollen-inferred Holocene vegetation and climate histories in Taro Co, southwestern Tibetan Plateau. Chinese Science Bulletin, 59(31): 4101-4114.
Ma, R., Duan, H., Hu, C., Feng, X., Li, A., Ju, W., Jiang, J. and Yang, G., 2010. A half-century of changes in China's lakes: Global warming or human influence? Geophys. Res. Lett., 37(24): L24106.
Ma, Y., Xu, N., Sun, J., Wang, X.H., Yang, F. and Li, S., 2019b. Estimating water levels and volumes of lakes dated back to the 1980s using Landsat imagery and photon-counting lidar datasets. Remote Sensing of Environment, 232: 111287.
Mao, D., Wang, Z., Yang, H., Li, H., Thompson, J., Li, L., Song, K., Chen, B., Gao, H. and Wu, J., 2018. Impacts of Climate Change on Tibetan Lakes: Patterns and Processes. Remote Sensing, 10(3): 358.
Markus, T., Neumann, T., Martino, A., Abdalati, W., Brunt, K., Csatho, B., Farrell, S., Fricker, H., Gardner, A., Harding, D., Jasinski, M., Kwok, R., Magruder, L., Lubin, D., Luthcke, S., Morison, J., Nelson, R., Neuenschwander, A., Palm, S., Popescu, S., Shum, C.K., Schutz, B.E., Smith, B., Yang, Y. and Zwally, J., 2017. The Ice, Cloud, and land Elevation Satellite-2 (ICESat-2): Science requirements, concept, and implementation. Remote Sensing of Environment, 190: 260-273.
Martens, B., Miralles, D.G., Lievens, H., van der Schalie, R., de Jeu, R.A.M., Fernández-Prieto, D., Beck, H.E., Dorigo, W.A. and Verhoest, N.E.C., 2017. GLEAM v3: satellite-based land evaporation and root-zone soil moisture. Geosci. Model Dev., 10(5): 1903-1925.
Marzeion, B., Jarosch, A.H. and Hofer, M., 2012. Past and future sea-level change from the surface mass balance of glaciers. The Cryosphere, 6(6): 1295-1322.
Maussion, F., Scherer, D., Mölg, T., Collier, E., Curio, J. and Finkelnburg, R., 2014. Precipitation Seasonality and Variability over the Tibetan Plateau as Resolved by the High Asia Reanalysis. Journal of Climate, 27(5): 1910-1927.
McFeeters, S., 2013. Using the Normalized Difference Water Index (NDWI) within a Geographic Information System to Detect Swimming Pools for Mosquito Abatement: A Practical Approach. Remote Sensing, 5(7): 3544-3561.
McFeeters, S.K., 1996. The use of the normalized difference water index (NDWI) in the delineation of open water features. International Journal of Remote Sensing, 17(7): 1425−1432.
McGill, M., Markus, T., Scott, V.S. and Neumann, T., 2013. The Multiple Altimeter Beam Experimental Lidar (MABEL): An Airborne Simulator for the ICESat-2 Mission. Journal of Atmospheric and Oceanic Technology, 30(2): 345-352.
Meng, F., Su, F., Li, Y. and Tong, K., 2020. Changes in terrestrial water storage during 2003–2014 and possible causes in Tibetan Plateau. Journal of Geophysical Research: Atmospheres, 124(6): 2909-2931.
Messager, M.L., Lehner, B., Grill, G., Nedeva, I. and Schmitt, O., 2016. Estimating the volume and age of water stored in global lakes using a geo-statistical approach. Nat Commun, 7: 13603.
Micklin, P.P., 1988. Desiccation of the aral sea: a water management disaster in the soviet union. Science, 241(4870): 1170-1176.

Miles, K.E., Willis, I.C., Benedek, C.L., Williamson, A.G. and Tedesco, M., 2017. Toward Monitoring Surface and Subsurface Lakes on the Greenland Ice Sheet Using Sentinel-1 SAR and Landsat-8 OLI Imagery. Frontiers in Earth Science, 5: 58.
Mountain Research Initiative, E.D.W.W.G., 2015. Elevation-dependent warming in mountain regions of the world. Nature Clim. Change, 5(5): 424-430.
O'Reilly, C.M., Sharma, S., Gray, D.K., Hampton, S.E., Read, J.S., Rowley, R.J., Schneider, P., Lenters, J.D., McIntyre, P.B., Kraemer, B.M., Weyhenmeyer, G.A., Straile, D., Dong, B., Adrian, R., Allan, M.G., Anneville, O., Arvola, L., Austin, J., Bailey, J.L., Baron, J.S., Brookes, J.D., de Eyto, E., Dokulil, M.T., Hamilton, D.P., Havens, K., Hetherington, A.L., Higgins, S.N., Hook, S., Izmest'eva, L.R., Joehnk, K.D., Kangur, K., Kasprzak, P., Kumagai, M., Kuusisto, E., Leshkevich, G., Livingstone, D.M., MacIntyre, S., May, L., Melack, J.M., Mueller-Navarra, D.C., Naumenko, M., Noges, P., Noges, T., North, R.P., Plisnier, P.-D., Rigosi, A., Rimmer, A., Rogora, M., Rudstam, L.G., Rusak, J.A., Salmaso, N., Samal, N.R., Schindler, D.E., Schladow, S.G., Schmid, M., Schmidt, S.R., Silow, E., Soylu, M.E., Teubner, K., Verburg, P., Voutilainen, A., Watkinson, A., Williamson, C.E. and Zhang, G., 2015. Rapid and highly variable warming of lake surface waters around the globe. Geophysical Research Letters, 42(24): 10773-10781.
Oelke, C. and Zhang, T., 2007. Modeling the Active-Layer Depth over the Tibetan Plateau. Arctic, Antarctic, and Alpine Research, 39(4): 714-722.
Otsu, N., 1979. A Threshold Selection Method from Gray-Level Histograms. IEEE Transactions on Systems, Man and Cybernetics, 9(1): 62−66.
Pei, J., Wang, L., Xu, W., Kurz, D.J., Geng, J., Fang, H., Guo, X. and Niu, Z., 2019. Recovered Tibetan antelope at risk again. Science, 366(6462): 194-194.
Pekel, J.-F., Cottam, A., Gorelick, N. and Belward, A.S., 2016. High-resolution mapping of global surface water and its long-term changes. Nature, 540: 418−422.
Pepin, N., Deng, H., Zhang, H., Zhang, F., Kang, S. and Yao, T., 2019. An Examination of Temperature Trends at High Elevations Across the Tibetan Plateau: The Use of MODIS LST to Understand Patterns of Elevation-Dependent Warming. Journal of Geophysical Research: Atmospheres, 124(11): 5738-5756.
Pham-Duc, B., Sylvestre, F., Papa, F., Frappart, F., Bouchez, C. and Crétaux, J.-F., 2020. The Lake Chad hydrology under current climate change. Scientific Reports, 10(1): 5498.
Phan, V.H., Lindenbergh, R. and Menenti, M., 2012. ICESat derived elevation changes of Tibetan lakes between 2003 and 2009. International Journal of Applied Earth Observation and Geoinformation, 17: 12−22.
Qiao, B., Zhu, L., Wang, J., Ju, J., Ma, Q., Huang, L., Chen, H., Liu, C. and Xu, T., 2019a. Estimation of lake water storage and changes based on bathymetric data and altimetry data and the association with climate change in the central Tibetan Plateau. Journal of Hydrology, 578: 124052.
Qiao, B., Zhu, L. and Yang, R., 2019b. Temporal-spatial differences in lake water storage changes and their links to climate change throughout the Tibetan Plateau. Remote Sensing of Environment, 222: 232-243.
Qin, J., Yang, K., Liang, S. and Guo, X., 2009. The altitudinal dependence of recent rapid warming over the Tibetan Plateau. Climatic Change, 97(1): 321-327.
Qiu, J., 2008. The Third Pole. Nature, 454(7203): 393-396.
Qiu, Y., Xie, P., Leppäranta, M., Wang, X., Lemmetyinen, J., Lin, H. and Shi, L., 2019. MODIS-based Daily Lake Ice Extent and Coverage dataset for Tibetan Plateau. Big Earth Data, 3(2): 170-185.
Radić, V., Bliss, A., Beedlow, A.C., Hock, R., Miles, E. and Cogley, J.G., 2014. Regional and global projections of twenty-first century glacier mass changes in response to climate scenarios from global climate models. Climate Dynamics, 42(1-2): 37-58.
RGI-Consortium, 2017. Randolph glacier inventory–a dataset of global glacier outlines: Version 6.0: technical report, global land ice measurements from space, Colorado, USA. Digital Media.
Rodell, M., Velicogna, I. and Famiglietti, J.S., 2009. Satellite-based estimates of groundwater depletion in India. Nature, 460(7258): 999-1002.
Roy, D.P., Ju, J., Kline, K., Scaramuzza, P.L., Kovalskyy, V., Hansen, M., Loveland, T.R., Vermote, E. and Zhang, C., 2010. Web-enabled Landsat Data (WELD): Landsat ETM+ composited mosaics of the conterminous United States. Remote Sensing of Environment, 114(1): 35-49.
Roy, D.P., Wulder, M.A., Loveland, T.R., C.E, W., Allen, R.G., Anderson, M.C., Helder, D., Irons, J.R., Johnson, D.M., Kennedy, R., Scambos, T.A., Schaaf, C.B., Schott, J.R., Sheng, Y., Vermote, E.F., Belward, A.S., Bindschadler, R., Cohen, W.B., Gao, F., Hipple, J.D., Hostert, P., Huntington, J., Justice, C.O., Kilic, A., Kovalskyy, V., Lee, Z.P., Lymburner, L., Masek, J.G., McCorkel, J., Shuai, Y., Trezza, R., Vogelmann, J., Wynne, R.H. and Zhu, Z., 2014. Landsat-8: Science and product vision for terrestrial global change research. Remote Sensing of Environment, 145: 154−172.
Ruosteenoja, K., 1986. The date of break-up of lake ice as a climatic index. Geophysica, 22(1-2): 89-99.
Schneider, U., Becker, A., Finger, P., Meyer-Christoffer, A., Ziese, M. and Rudolf, B., 2014. GPCC's new land surface precipitation climatology based on quality-controlled in situ data and its role in quantifying the global water cycle. v. 115.

Schutz, B.E., Zwally, H.J., Shuman, C.A., Hancock, D. and DiMarzio, J.P., 2005. Overview of the ICESat Mission. Geophys. Res. Lett., 32: L21S01.
Shamsudduha, M., Taylor, R.G. and Longuevergne, L., 2012. Monitoring groundwater storage changes in the highly seasonal humid tropics: Validation of GRACE measurements in the Bengal Basin. Water Resources Research, 48(2): W02508.
Sharma, S., Blagrave, K., Magnuson, J.J., O'Reilly, C.M., Oliver, S., Batt, R.D., Magee, M.R., Straile, D., Weyhenmeyer, G.A., Winslow, L. and Woolway, R.I., 2019. Widespread loss of lake ice around the Northern Hemisphere in a warming world. Nature Climate Change, 9: 227-231.
Sharma, S., Gray, D.K., Read, J.S., O'Reilly, C.M., Schneider, P., Qudrat, A., Gries, C., Stefanoff, S., Hampton, S.E., Hook, S., Lenters, J.D., Livingstone, D.M., McIntyre, P.B., Adrian, R., Allan, M.G., Anneville, O., Arvola, L., Austin, J., Bailey, J., Baron, J.S., Brookes, J., Chen, Y., Daly, R., Dokulil, M., Dong, B., Ewing, K., de Eyto, E., Hamilton, D., Havens, K., Haydon, S., Hetzenauer, H., Heneberry, J., Hetherington, A.L., Higgins, S.N., Hixson, E., Izmest'eva, L.R., Jones, B.M., Kangur, K., Kasprzak, P., Köster, O., Kraemer, B.M., Kumagai, M., Kuusisto, E., Leshkevich, G., May, L., MacIntyre, S., Müller-Navarra, D., Naumenko, M., Noges, P., Noges, T., Niederhauser, P., North, R.P., Paterson, A.M., Plisnier, P.-D., Rigosi, A., Rimmer, A., Rogora, M., Rudstam, L., Rusak, J.A., Salmaso, N., Samal, N.R., Schindler, D.E., Schladow, G., Schmidt, S.R., Schultz, T., Silow, E.A., Straile, D., Teubner, K., Verburg, P., Voutilainen, A., Watkinson, A., Weyhenmeyer, G.A., Williamson, C.E. and Woo, K.H., 2015. A global database of lake surface temperatures collected by in situ and satellite methods from 1985–2009. Scientific Data, 2: 150008.
Sheng, Y., Song, C., Wang, J., Lyons, E.A., Knox, B.R., Cox, J.S. and Gao, F., 2016. Representative lake water extent mapping at continental scales using multi-temporal Landsat-8 imagery. Remote Sensing of Environment, 185: 129-141.
Son, J.-H., Seo, K.-H. and Wang, B., 2019. Dynamical Control of the Tibetan Plateau on the East Asian Summer Monsoon. Geophysical Research Letters, 46(13): 7672-7679.
Song, C., Huang, B. and Ke, L., 2013. Modeling and analysis of lake water storage changes on the Tibetan Plateau using multi-mission satellite data. Remote Sensing of Environment, 135: 25–35.
Song, C., Huang, B., Ke, L. and Richards, K.S., 2014a. Remote sensing of alpine lake water environment changes on the Tibetan Plateau and surroundings: A review. ISPRS Journal of Photogrammetry and Remote Sensing, 92: 26-37.
Song, C., Huang, B., Richards, K., Ke, L. and Hien, V.P., 2014b. Accelerated lake expansion on the Tibetan Plateau in the 2000s: Induced by glacial melting or other processes? Water Resources Research, 50: 3170–3186.
Strozzi, T., Wiesmann, A., Kääb, A., Joshi, S. and Mool, P., 2012. Glacial lake mapping with very high resolution satellite SAR data. Natural Hazards and Earth System Science, 12(8): 2487-2498.
Sun, J. and Yang, K., 2020. Why the western Tibetan Plateau has become wetter since the mid-1990s? Journal of Climate: Under Review.
Sun, J., Zhou, T., Liu, M., Chen, Y., Shang, H., Zhu, L., Shedayi, A.A., Yu, H., Cheng, G., Liu, G., Xu, M., Deng, W., Fan, J., Lu, X. and Sha, Y., 2018. Linkages of the dynamics of glaciers and lakes with the climate elements over the Tibetan Plateau. Earth-Science Reviews, 185: 308-324.
Swenson, S., Chambers, D. and Wahr, J., 2008. Estimating geocenter variations from a combination of GRACE and ocean model output. Journal of Geophysical Research: Solid Earth, 113(B8): B08410.
Tao, S., Fang, J., Zhao, X., Zhao, S., Shen, H., Hu, H., Tang, Z., Wang, Z. and Guo, Q., 2015. Rapid loss of lakes on the Mongolian Plateau. Proceedings of the National Academy of Sciences, 112(7): 2281–2286.
Tapley, B.D., Bettadpur, S., Ries, J.C., Thompson, P.F. and Watkins, M.M., 2004. GRACE measurements of mass variability in the Earth system. Science, 305(5683): 503-505.
Tapley, B.D., Watkins, M.M., Flechtner, F., Reigber, C., Bettadpur, S., Rodell, M., Sasgen, I., Famiglietti, J.S., Landerer, F.W., Chambers, D.P., Reager, J.T., Gardner, A.S., Save, H., Ivins, E.R., Swenson, S.C., Boening, C., Dahle, C., Wiese, D.N., Dobslaw, H., Tamisiea, M.E. and Velicogna, I., 2019. Contributions of GRACE to understanding climate change. Nature Climate Change, 9: 358-369.
Taube, C.M., 2000. Three Methods for Computing the Volume of a Lake. Chapter 12 in Schneider, James C. (ed.) 2000. Manual of fisheries survey methods II: with periodic updates. Michigan Department of Natural Resources, Fisheries Special Report 25, Ann Arbor. In: J. C. (Editor). Manual of fisheries survey methods II: with periodic updates.
Tong, K., Su, F. and Xu, B., 2016. Quantifying the contribution of glacier-melt water in the expansion of the largest lake in Tibet. J Geophys Res, 121: 11158-11173.
Tong, K., Su, F., Yang, D., Zhang, L. and Hao, Z., 2014. Tibetan Plateau precipitation as depicted by gauge observations, reanalyses and satellite retrievals. International Journal of Climatology, 34(2): 265-285.
Treichler, D., Kääb, A., Salzmann, N. and Xu, C.-Y., 2019. Recent glacier and lake changes in High Mountain Asia and their relation to precipitation changes. The Cryosphere, 13(11): 2977-3005.

Verpoorter, C., Kutser, T., Seekell, D.A. and Tranvik, L.J., 2014. A Global Inventory of Lakes Based on High-Resolution Satellite Imagery. Geophysical Research Letters, 41: 6396−6402.
Wahr, J., Molenaar, M. and Bryan, F., 1998. Time variability of the Earth's gravity field: Hydrological and oceanic effects and their possible detection using GRACE. Journal of Geophysical Research: Solid Earth, 103(B12): 30205-30229.
Wan, W., Long, D., Hong, Y., Ma, Y., Yuan, Y., Xiao, P., Duan, H., Han, Z. and Gu, X., 2016. A lake data set for the Tibetan Plateau from the 1960s, 2005, and 2014. Scientific Data, 3: 160039.
Wan, W., Xiao, P., Feng, X., Li, H., Ma, R., Duan, H. and Zhao, L., 2014. Monitoring lake changes of Qinghai-Tibetan Plateau over the past 30 years using satellite remote sensing data. Chinese Science Bulletin, 59(10): 1021−1035.
Wan, W., Zhao, L., Xie, H., Liu, B., Li, H., Cui, Y., Ma, Y. and Hong, Y., 2018. Lake Surface Water Temperature Change Over the Tibetan Plateau From 2001 to 2015: A Sensitive Indicator of the Warming Climate. Geophysical Research Letters, 45(20): 11177-11186.
Wang, B., Liu, J., Kim, H.-J., Webster, P.J., Yim, S.-Y. and Xiang, B., 2013. Northern Hemisphere summer monsoon intensified by mega-El Niño/southern oscillation and Atlantic multidecadal oscillation. Proceedings of the National Academy of Sciences of the United States of America, 110(14): 5347−5352.
Wang, B., Ma, Y., Wang, Y., Su, Z. and Ma, W., 2019. Significant differences exist in lake-atmosphere interactions and the evaporation rates of high-elevation small and large lakes. Journal of Hydrology, 573: 220-234.
Wang, J., Sheng, Y. and Wada, Y., 2017. Little impact of the Three Gorges Dam on recent decadal lake decline across China's Yangtze Plain. Water Resources Research, 53(5): 3854-3877.
Wang, J., Zhu, L., Daut, G., Ju, J., Lin, X., Wang, Y. and Zhen, X., 2009. Investigation of bathymetry and water quality of Lake Nam Co, the largest lake on the central Tibetan Plateau, China. Limnology, 10(2): 149-158.
Wang, Q., Yi, S. and Sun, W., 2016. The changing pattern of lake and its contribution to increased mass in the Tibetan Plateau derived from GRACE and ICESat data. Geophysical Journal International, 207: 528-541.
Wang, W., Lee, X., Xiao, W., Liu, S., Schultz, N., Wang, Y., Zhang, M. and Zhao, L., 2018a. Global lake evaporation accelerated by changes in surface energy allocation in a warmer climate. Nature Geoscience, 11: 410-414.
Wang, X., Pang, G. and Yang, M., 2018b. Precipitation over the Tibetan Plateau during recent decades: a review based on observations and simulations. International Journal of Climatology, 38(3): 1116-1131.
Wangchuk, S., Bolch, T. and Zawadzki, J., 2019. Towards automated mapping and monitoring of potentially dangerous glacial lakes in Bhutan Himalaya using Sentinel-1 Synthetic Aperture Radar data International Journal of Remote Sensing, 40(12): 4642-4667.
Watson, C.S., King, O., Miles, E.S. and Quincey, D.J., 2018. Optimising NDWI supraglacial pond classification on Himalayan debris-covered glaciers. Remote Sensing of Environment, 217: 414-425.
Weber, H., Riffler, M., Nõges, T. and Wunderle, S., 2016. Lake ice phenology from AVHRR data for European lakes: An automated two-step extraction method. Remote Sensing of Environment, 174: 329-340.
Woolway, R.I. and Merchant, C.J., 2017. Amplified surface temperature response of cold, deep lakes to inter-annual air temperature variability. Scientific Reports, 7(1): 4130.
Wortmann, M., Bolch, T., Menz, C., Tong, J. and Krysanova, V., 2018. Comparison and Correction of High-Mountain Precipitation Data Based on Glacio-Hydrological Modeling in the Tarim River Headwaters (High Asia). Journal of Hydrometeorology, 19(5): 777-801.
Wu, G., Liu, Y., Wang, T., Wan, R., Liu, X., Li, W., Wang, Z., Zhang, Q., Duan, A. and Liang, X., 2007. The Influence of Mechanical and Thermal Forcing by the Tibetan Plateau on Asian Climate. Journal of Hydrometeorology, 8(4): 770-789.
Wu, Q., Hou, Y., Yun, H. and Liu, Y., 2014. Changes in active-layer thickness and near-surface permafrost between 2002 and 2012 in alpine ecosystems, Qinghai-Xizang (Tibet) Plateau, China. Global and Planetary Change, 124: 149-155.
Wu, Y., Huang, A., Yang, B., Dong, G., Wen, L., Lazhu, Zhang, Z., Fu, Z., Zhu, X., Zhang, X. and Cai, S., 2019. Numerical study on the climatic effect of the lake clusters over Tibetan Plateau in summer. Climate Dynamics, 53(9-10): 5215-5236.
Wulder, M.A., Loveland, T.R., Roy, D.P., Crawford, C.J., Masek, J.G., Woodcock, C.E., Allen, R.G., Anderson, M.C., Belward, A.S., Cohen, W.B., Dwyer, J., Erb, A., Gao, F., Griffiths, P., Helder, D., Hermosilla, T., Hipple, J.D., Hostert, P., Hughes, M.J., Huntington, J., Johnson, D.M., Kennedy, R., Kilic, A., Li, Z., Lymburner, L., McCorkel, J., Pahlevan, N., Scambos, T.A., Schaaf, C., Schott, J.R., Sheng, Y., Storey, J., Vermote, E., Vogelmann, J., White, J.C., Wynne, R.H. and Zhu, Z., 2019. Current status of Landsat program, science, and applications. Remote Sensing of Environment, 225: 127-147.
Xiang, L., Wang, H., Steffen, H., Wu, P., Jia, L., Jiang, L. and Shen, Q., 2016. Groundwater storage changes in the Tibetan Plateau and adjacent areas revealed from GRACE satellite gravity data. Earth and Planetary Science Letters, 449: 228-239.

Xu, H., 2006. Modification of normalised difference water index (NDWI) to enhance open water features in remotely sensed imagery. International Journal of Remote Sensing, 27(14): 3025−3033.
Xu, X., Lu, C., Shi, X. and Gao, S., 2008. World water tower: An atmospheric perspective. Geophysical Research Letters, 35(20): L20815.
Yamazaki, D., Trigg, M.A. and Ikeshima, D., 2015. Development of a global ~ 90 m water body map using multi-temporal Landsat images. Remote Sensing of Environment, 171: 337−351.
Yan, F., Sillanpää, M., Kang, S., Aho, K.S., Qu, B., Wei, D., Li, X., Li, C. and Raymond, P.A., 2018. Lakes on the Tibetan Plateau as Conduits of Greenhouse Gases to the Atmosphere. Journal of Geophysical Research: Biogeosciences, 123(7): 2091-2103.
Yan, L. and Zheng, M., 2015. Influence of climate change on saline lakes of the Tibet Plateau, 1973–2010. Geomorphology, 246: 68-78.
Yang, K., Ding, B., Qin, J., Tang, W., Lu, N. and Lin, C., 2012. Can aerosol loading explain the solar dimming over the Tibetan Plateau? Geophysical Research Letters, 39(20): L20710.
Yang, K., Lu, H., Yue, S., Zhang, G., Lei, Y., Zhu, L. and Wang, W., 2018. Quantifying recent precipitation change and predicting lake expansion in the Inner Tibetan Plateau. Climatic Change, 147(1-2): 149-163.
Yang, K., Wu, H., Qin, J., Lin, C., Tang, W. and Chen, Y., 2014. Recent climate changes over the Tibetan Plateau and their impacts on energy and water cycle: A review. Global and Planetary Change, 112: 79−91.
Yang, K., Yao, F., Wang, J., Luo, J., Shen, Z., Wang, C. and Song, C., 2017a. Recent dynamics of alpine lakes on the endorheic Changtang Plateau from multi-mission satellite data. Journal of Hydrology, 552: 633-645.
Yang, K., Ye, B., Zhou, D., Wu, B., Foken, T., Qin, J. and Zhou, Z., 2011. Response of hydrological cycle to recent climate changes in the Tibetan Plateau. Climatic Change, 109(3): 517−534.
Yang, M., Nelson, F.E., Shiklomanov, N.I., Guo, D. and Wan, G., 2010. Permafrost degradation and its environmental effects on the Tibetan Plateau: A review of recent research. Earth-Science Reviews, 103(1-2): 31-44.
Yang, R., Zhu, L., Wang, J., Ju, J., Ma, Q., Turner, F. and Guo, Y., 2017b. Spatiotemporal variations in volume of closed lakes on the Tibetan Plateau and their climatic responses from 1976 to 2013. Climatic Change, 140(3): 621-633.
Yang, X. and Lu, X., 2014. Drastic change in China's lakes and reservoirs over the past decades. Scientific Reports, 4: 6041.
Yang, Y., Liu, Y., Zhou, M., Zhang, S., Zhan, W., Sun, C. and Duan, Y., 2015. Landsat 8 OLI image based terrestrial water extraction from heterogeneous backgrounds using a reflectance homogenization approach. Remote Sensing of Environment, 171: 14−32.
Yang, Y., Wu, Q., Jin, H., Wang, Q., Huang, Y., Luo, D., Gao, S. and Jin, X., 2019. Delineating the hydrological processes and hydraulic connectivities under permafrost degradation on Northeastern Qinghai-Tibet Plateau, China. Journal of Hydrology, 569: 359-372.
Yao, F., Wang, J., Wang, C. and Crétaux, J.-F., 2019. Constructing long-term high-frequency time series of global lake and reservoir areas using Landsat imagery. Remote Sensing of Environment, 232: 111210.
Yao, F., Wang, J., Yang, K., Wang, C., Walter, B. and Cretaux, J.-F., 2018. Lake storage variation on the endorheic Tibetan Plateau and its attribution to climate change since the new millennium. Environmental Research Letters, 13(6): 064011.
Yao, T., Thompson, L., Yang, W., Yu, W., Gao, Y., Guo, X., Yang, X., Duan, K., Zhao, H., Xu, B., Pu, J., Lu, A., Xiang, Y., Kattel, D.B. and Joswiak, D., 2012. Different glacier status with atmospheric circulations in Tibetan Plateau and surroundings. Nature Climate Change, 2(9): 663-667.
Yao, X., Sun, M., Gong, P., Liu, B., Li, X., An, L. and Ma, C., 2016. Overflow probability of the Salt Lake in Hoh Xil Region. Acta Geographica Sinica, 71(9): 1520-1527.
Yatagai, A., Kamiguchi, K., Arakawa, O., Hamada, A., Yasutomi, N. and Kitoh, A., 2012. APHRODITE: Constructing a Long-Term Daily Gridded Precipitation Dataset for Asia Based on a Dense Network of Rain Gauges. Bulletin of the American Meteorological Society, 93(9): 1401-1415.
Yi, S., Heki, K. and Qian, A., 2017. Acceleration in the Global Mean Sea Level Rise: 2005–2015. Geophysical Research Letters, 44(23): 11905-11913.
Yi, S., Wang, Q. and Sun, W., 2016. Basin mass dynamic changes in China from GRACE based on a multi-basin inversion method. Journal of Geophysical Research: Solid Earth, 121: 3782-3803.
Yu, J., Zhang, G., Yao, T., Xie, H., Zhang, H., Ke, C. and Yao, R., 2016. Developing daily cloud-free snow composite products from MODIS Terra-Aqua and IMS for the Tibetan Plateau. IEEE Transactions on Geoscience and Remote Sensing, 54(4): 2171−2180.
Zhang, B., Wu, Y., Zhu, L., Wang, J., Li, J. and Chen, D., 2011a. Estimation and trend detection of water storage at Nam Co Lake, central Tibetan Plateau. Journal of Hydrology, 405(1-2): 161−170.
Zhang, C., Tang, Q., Chen, D., J. van der Ent, R., Liu, X., Li, W. and Haile, G.G., 2019a. Moisture Source Changes Contributed to Different Precipitation Changes over the Northern and Southern Tibetan Plateau. Journal of Hydrometeorology, 20(2): 217-229.

Zhang, G., Chen, W., Li, G., Yang, W., Yi, S. and Luo, W., 2020a. Lake water and glacier mass gains in the northwestern Tibetan Plateau observed from multi-sensor remote sensing data: Implication of an enhanced hydrological cycle. Remote Sensing of Environment, 237: 111554.
Zhang, G., Chen, W. and Xie, H., 2019b. Tibetan Plateau's lake level and volume changes from NASA's ICESat/ICESat-2 and Landsat missions. Geophysical Research Letters, 46: 13107–13118.
Zhang, G., Chen, W., Zheng, G., Xie, H. and Shum, C.K., 2020b. Are China's water bodies (lakes) underestimated? Proceedings of the National Academy of Sciences, 117(112): 6308-6309.
Zhang, G., Li, J. and Zheng, G., 2017a. Lake-area mapping in the Tibetan Plateau: an evaluation of data and methods. International Journal of Remote Sensing, 38(3): 742-772.
Zhang, G., Luo, W., Chen, W. and Zheng, G., 2019c. A robust but variable lake expansion on the Tibetan Plateau. Science Bulletin, 64(18): 1306-1309.
Zhang, G., Xie, H., Duan, S., Tian, M. and Yi, D., 2011b. Water level variation of Lake Qinghai from satellite and in situ measurements under climate change. Journal of Applied Remote Sensing, 5: 053532.
Zhang, G., Xie, H., Kang, S., Yi, D. and Ackley, S., 2011c. Monitoring lake level changes on the Tibetan Plateau using ICESat altimetry data (2003−2009). Remote Sensing of Environment, 115(7): 1733−1742.
Zhang, G., Xie, H., Yao, T. and Kang, S., 2013a. Water balance estimates of ten greatest lakes in China using ICESat and Landsat data. Chinese Science Bulletin, 58(31): 3815−3829.
Zhang, G., Yao, T., Chen, W., Zheng, G., Shum, C.K., Yang, K., Piao, S., Sheng, Y., Yi, S., Li, J., O'Reilly, C.M., Qi, S., Shen, S.S.P., Zhang, H. and Jia, Y., 2019d. Regional differences of lake evolution across China during 1960s–2015 and its natural and anthropogenic causes. Remote Sensing of Environment, 221: 386-404.
Zhang, G., Yao, T., Piao, S., Bolch, T., Xie, H., Chen, D., Gao, Y., O'Reilly, C.M., Shum, C.K., Yang, K., Yi, S., Lei, Y., Wang, W., He, Y., Shang, K., Yang, X. and Zhang, H., 2017b. Extensive and drastically different alpine lake changes on Asia's high plateaus during the past four decades. Geophysical Research Letters, 44(1): 252-260.
Zhang, G., Yao, T., Shum, C.K., Yi, S., Yang, K., Xie, H., Feng, W., Bolch, T., Wang, L., Behrangi, A., Zhang, H., Wang, W., Xiang, Y. and Yu, J., 2017c. Lake volume and groundwater storage variations in Tibetan Plateau's endorheic basin. Geophysical Research Letters, 44(11): 5550-5560.
Zhang, G., Yao, T., Xie, H., Kang, S. and Lei, Y., 2013b. Increased mass over the Tibetan Plateau: From lakes or glaciers? Geophysical Research Letters, 40(10): 2125−2130.
Zhang, G., Yao, T., Xie, H., Qin, J., Ye, Q., Dai, Y. and Guo, R., 2014a. Estimating surface temperature changes of lakes in the Tibetan Plateau using MODIS LST data. Journal of Geophysical Research: Atmospheres, 119(14): 8552−8567.
Zhang, G., Yao, T., Xie, H., Zhang, K. and Zhu, F., 2014b. Lakes' state and abundance across the Tibetan Plateau. Chinese Science Bulletin, 59(24): 3010−3021.
Zhang, G., Zheng, G., Gao, Y., Xiang, Y., Lei, Y. and Li, J., 2017d. Automated water classification in the Tibetan Plateau using Chinese GF-1 WFV data. Photogrammetric Engineering & Remote Sensing, 83(3): 33-43.
Zhang, Y., Zhang, G. and Zhu, T., 2020c. Seasonal cycles of lakes on the Tibetan Plateau detected by Sentinel-1 SAR data. Science of the Total Environment, 703: 135563.
Zhao, W., Amelung, F., Doin, M.-P., Dixon, T.H., Wdowinski, S. and Lin, G., 2016. InSAR observations of lake loading at Yangzhuoyong Lake, Tibet: Constraints on crustal elasticity. Earth and Planetary Science Letters, 449: 240-245.
Zhong, L., Ma, Y., Xue, Y. and Piao, S., 2019. Climate Change Trends and Impacts on Vegetation Greening Over the Tibetan Plateau. Journal of Geophysical Research: Atmospheres, 124(14): 7540-7552.
Zhou, J., Wang, L., Zhang, Y., Guo, Y., Li, X. and Liu, W., 2015. Exploring the water storage changes in the largest lake (Selin Co) over the Tibetan Plateau during 2003–2012 from a basin-wide hydrological modeling. Water Resources Research, 51(10): 8060−8086.
Zhou, Y., Hu, J., Li, Z., Li, J., Zhao, R. and Ding, X., 2019. Quantifying glacier mass change and its contribution to lake growths in Central Kunlun during 2000-2015 from multi-source remote sensing data. Journal of Hydrology, 570: 38-50.
Zhu, L., Jin, J., Liu, X., Tian, L. and Zhang, Q., 2018. Simulations of the Impact of Lakes on Local and Regional Climate Over the Tibetan Plateau. Atmosphere-Ocean, 56(4): 230-239.
Zou, Z., Xiao, X., Dong, J., Qin, Y., Doughty, R.B., Menarguez, M.A., Zhang, G. and Wang, J., 2018. Divergent trends of open-surface water body area in the contiguous United States from 1984 to 2016. Proceedings of the National Academy of Sciences, 115(15): 3810-3815.